A Multi-Objective Optimisation on Agri-PV Systems

SET Master Thesis

Jeanne Ballaguy

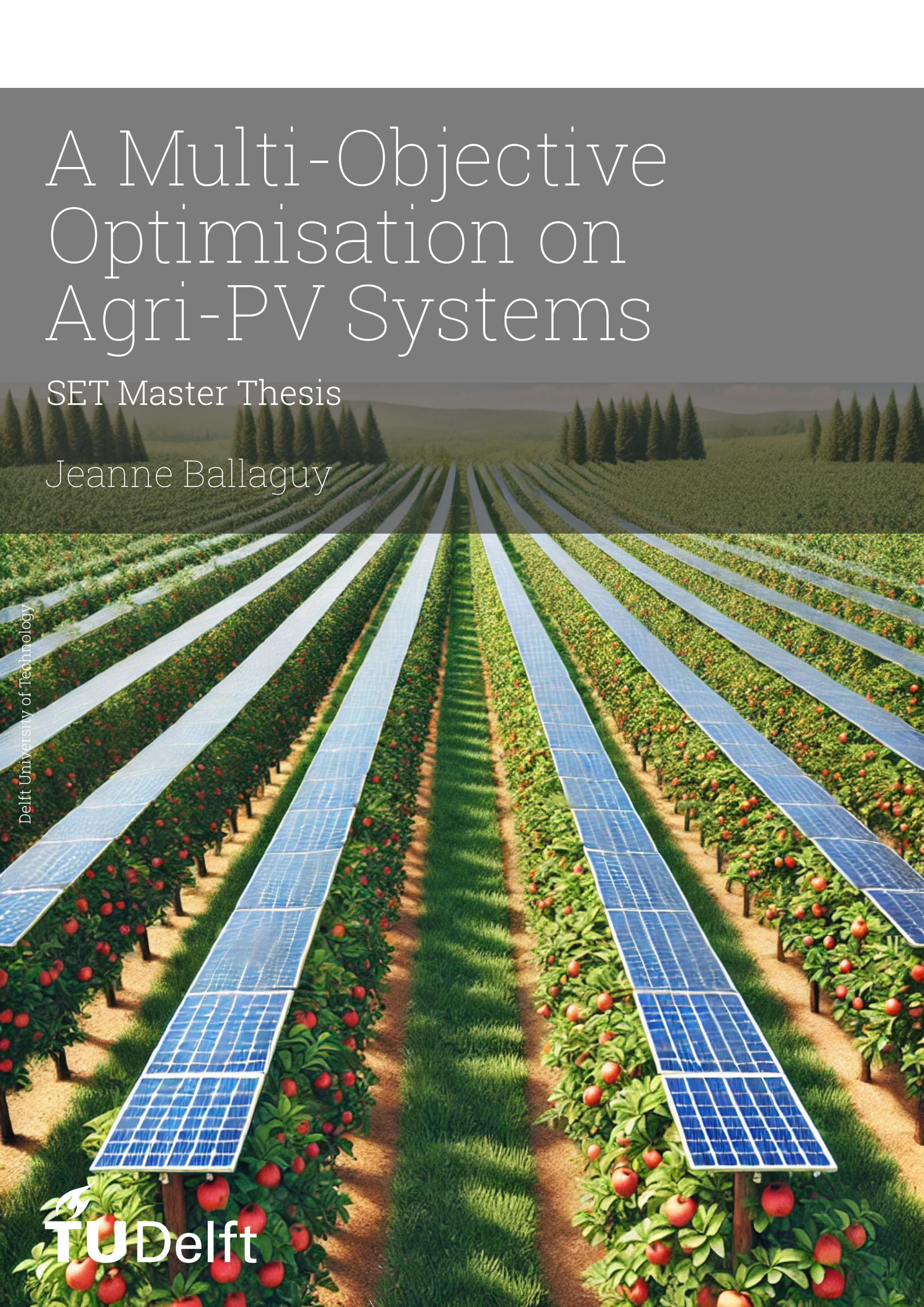

Delft University of Technology

TU Delft

A Multi-Objective Optimisation on Agri-PV Systems

SET Master Thesis

by

Jeanne Ballaguy

in partial fulfilment to obtain the degree of Master of Science in Sustainable Energy technology at the Delft University of Technology, to be defended publicly on 8th of July, 2024 at 1 PM.

Main Supervisor:	H. Ziar
Daily supervisor:	A. Katsikogiannis
Project Duration:	November, 2023 - July, 2024
Faculty:	Faculty of EEMCS, Delft

An electronic version of this thesis is available at http://repository.tudelft.nl/.

Cover: Image generated by DALL-E

TU Delft

Abstract

This thesis investigates the optimisation of fixed-tilt bifacial agricultural photovoltaic (agri-PV) orchard systems using a multi-objective approach, focusing on maximising both crop Photosynthetically Active Radiation (PAR) and PV radiation. Due to the complexity of modelling agri-PV systems, advanced light simulation tools like Radiance, a backward ray-tracing software, were integrated into the study. Although effective, this software introduces significant computational intensity and stochastic behaviour.

The primary aims of this thesis were to develop an optimisation algorithm for such irradiation models and to optimise the system by maintaining separate objectives for crops and PV modules. This separation eliminates inter-connectivity between the conflicting metrics during the optimisation process. Additionally, a single-objective optimisation was conducted by summing the two conflicting objectives to assess the impact of this separation.

The research concluded that Bayesian optimisation with Gaussian Processes is most suitable due to its efficiency and ability to handle noise. Applied to an apple orchard case study in northern Italy, the algorithm demonstrated significant advantages over classical Radiance-based methods, achieving high accuracy in a fraction of the time. Results indicated that multi-objective optimisation offers more robust and informative solutions compared to single-objective optimisation.

In conclusion, this thesis enhances the understanding and optimisation of agri-PV systems, enabling quicker, more accurate analyses and providing practical solutions for farmers and other users.

Summary

This thesis investigates the optimisation of fixed-tilt bifacial agricultural photovoltaic (agri-PV) orchard systems using a multi-objective approach, focusing on maximising both crop Photosynthetically Active Radiation (PAR) and PV radiation. Agri-PV system are complex to model, thus necessitating advanced light simulation tools like those base on ray-tracing. Therefore, Radiance, a backward ray-tracing light simulation software was integrated in the study. However, using such software comes with the drawback that the simulations are very computationally intensive and introduce stochastic behaviour. The first aim of this thesis is to develop an optimisation algorithm for this kind of irradiation model. The second aim is to optimise the system by maintaining separate objectives for the crop and PV modules, thereby eliminating inter-connectivity between the two conflicting metrics during the optimisation process. To assess the impact of this separation, a single-objective optimisation is conducted by summing the two conflicting objective functions.

The research sought to answer three primary questions: identifying the most effective optimisation algorithm for integration with Radiance-based models, evaluating the advantages of optimisation assisted ray-tracing over classical Radiance-based ray-tracing, and comparing the performance of multi-objective versus single-objective optimisation in agri-PV systems.

After a literature review, it was determined that Bayesian optimisation with Gaussian Processes was most suitable due to its ability to deal with noise and most importantly its high efficiency, thus limiting the number of Radiance evaluations needed. The python package called Trieste is used and the optimisation algorithm is applied to a specific case study for an apple orchard in northern Italy. The design variables are tilt angle and cell gap factors (spacing between two solar cells on a module) and the radiation values are derived from sensors strategically positioned across the crops and pv panels.

Regarding the advantages of optimisation over classical Radiance, results demonstrated that the GP model could achieve 95% accuracy for the objective function(s) within just one hour, reaching up to 98% after only three hours, compared to over four days using classical Radiance ray-tracing. Furthermore, not only is the GP model accuracy high, but the same optimisation loop provided accurate optimal solution(s). Therefore, instead of taking four days using classical methods, Bayesian optimisation can obtain a high accuracy proxy model along with optimal agri-PV layouts in one hour.

Finally, it was concluded that for agri-PV systems, multi-objective optimisation is more beneficial than single-objective optimisation. It provides more information about the conflicting objectives, offers a broader choice of solutions, and is more robust to parameter changes.

In conclusion, this thesis makes a valuable contribution to optimising agri-PV systems, enhancing the general understanding of agri-PV systems with complex crop geometry and promoting their use. Furthermore, it allows multi-site and layout analysis in less than a day, compared to four days for one location and layout using solely Radiance, offering quick and comparable practical solutions to farmers and other users.

Contents

1

Introduction

1.1. Background

With the global population on the rise, the demand for both clean energy and food is escalating. Solar energy, recognised for its sustainability, plays a crucial role in addressing these energy needs but also poses significant land-use challenges. In regions with dense populations, the competition for land between energy production and agriculture is particularly high. Agricultural Photovoltaic (Agri-PV) systems offer a compelling solution by merging solar energy generation with agriculture on the same plot of land. These systems strategically place solar panels over crops to provide shade, minimise water evaporation, and generate renewable energy simultaneously. This dual approach not only optimises land use but also alleviates the effects of extreme weather, potentially enhances crop yields under certain conditions, and contributes to a sustainable energy future (Toledo and Scognamiglio, 2021).

Between 2011 and 2020, agri-PV installations have grown by a factor of almost 600 world wide, highlighting their growing acceptance and feasibility (Gorjian et al., 2022). Notably, research has advanced the practical and theoretical understanding of agri-PV, reinforcing its potential across various agricultural and solar energy integration.

Despite ongoing efforts to refine agri-PV layouts, achieving an optimal configuration is complex. The systems must balance the contradictory goals of maximising sunlight exposure for energy production and providing sufficient light for crop growth. Factors such as field characteristics, crop types, system geometries, and geographical locations add layers of complexity to system design. Moreover, varied parameters like photosynthetic performance, energy yield, land use efficiency, and economic viability demand careful consideration. Consequently, optimising an agri-PV system is inherently complex. Nonetheless, research, such as a study from Germany, demonstrates that with proper optimisation, land use efficiency could increase by 1.6 to 1.9 times in certain contexts (Beck et al., 2012). Optimising agri-PV systems is thus essential for enhancing both agricultural output and electricity generation.

Although optimisation of agri-PV systems is often carefully conducted to maximise land use efficiency, it can still compromise the investment in PV systems or lead to crop failure, as discussed by (Campana et al., 2021). This underscores the necessity for multi-objective optimisation approaches that evaluate performance metrics independently, catering to the distinct needs of crops and PV systems. (Mengi et al., 2023) conducted a multi-objective optimisation study with a crop-driven optimal solutions, and (Campana et al., 2021) developed a multi-objective optimisation model for vertically mounted agri-PV systems. However, these models use very simplified analytical light models and still employ an objective function that combines the interests of both crops and PV panels.

Using a simplified light model is problematic as agri-PV systems involve complex plant geometries, require diffuse light under solar panels for bifacial PV modules, and must account for Lambertian and specular reflections in the scene.

To the best of the author's knowledge, there is a crucial need for more research on the multi-objective

optimisation of agri-PV systems using accurate light models, such as ray-tracing based on the Monte Carlo approaches alongside independent performance metrics for each component of the system that have conflicting objectives.

1.2. Objectives and Research Questions

To address this research gap, this study aims to develop a multi-objective optimisation model combined to an accurate light simulation software, exemplified by Radiance. Radiance is a backward ray-tracing model and it will be employed throughout the study. To address the complexity of agri-PV systems, a multi-objective optimisation approach is utilised, where the crop objective and PV module objective are maintained separately throughout the optimisation process, thus eliminating any inter-connectivity during the optimisation between the metrics of agri-PV systems.

However, using a highly accurate ray-tracing model comes with considerable drawbacks. Indeed, not only are the simulations now a black-box problem (where the internal workings of a system are not accessible) with stochastic behaviour, the simulations also become very computationally intensive.

Regarding the multi-objective optimisation approach, the study will also in parallel optimise the same agri-PV system using single-objective optimisation, where the two objectives of crop yield and PV panel efficiency are combined, to assess the impact and differences of such approach.

The following research questions are thus enunciated:

1. Which optimisation algorithm is most effective for integration with Radiance-based ray-tracing models in agri-PV systems?
2. What are the advantages of using optimisation methodologies over classical Radiance based ray-tracing for agri-PV systems?
3. How does multi-objective optimisation compare to single-objective optimisation in agri-PV systems?

The research approach consists of first identifying a suitable optimisation algorithm that is compatible with Radiance and capable of handling multi-objective optimisation. Once the optimisation algorithm is selected, a model combining Radiance with this algorithm is created. Subsequently, an agri-PV system is modelled in Radiance, with all necessary objective functions and variables defined.

The next step involves comparing the results of the predictions provided by the optimisation algorithm with the classical, exact results from Radiance to assess the advantages of using optimisation methodologies. This comparison is facilitated using colour maps of the design space that represent the objective value throughout the area.

Moving forward, the two optimisation algorithms are compared based on certain criteria using the optimal solutions provided by both single and multi-objective optimisation, along with their respective sensitivity analyses.

1.3. Thesis Outline

The thesis is organised as follows. Chapter 2 provides a comprehensive literature review, identifying existing research gaps in agri-PV optimisation and setting the stage for exploring suitable multi-objective optimisation techniques. The methodology described in Chapter 3 details the simulation framework within which the model is valid, alongside the theoretical foundations of the optimisation algorithms developed, and the application of Bayesian optimisation for both single and multi-objective scenarios. The results are discussed in three chapters: Chapter 4 compares the optimisation models to the classical Radiance results, Chapter 5 presents the optimal solutions found by the two optimisation algorithms, and Chapter 6 compares the optimisation approaches based on specific criteria. Finally, Chapter 7 discusses the limitations of the research and future directions, and Chapter 8 concludes this thesis.

2

Literature Review

To ensure that this thesis is viewed as a comprehensive work concerning the literature review, the chapter details the important aspects of the topic providing important notions to understanding the current situation. Firstly, Section 2.1 presents the sate of the art of agri-PV systems, looking into the historical development and empirical insights, Section 2.1.1, the evolution and application of a commonly used performance metrics called Land Equivalent Ration (LER), Section 2.1.2 and Section 2.1.3 discusses current trends in agri-PV system optimisation. Secondly, Section 2.2 reviews various multi-objective optimisation algorithms (MOOAs), comparing their suitability for optimising agri-PV systems, particularly in handling computationally intensive simulations with Radiance.

2.1. State of the Art in Agri-PV Optimisation

Agri-PV systems represent an innovative integration of agriculture and PV technology, offering a dual-purpose solution to the increasing demands for land, energy, and food security. As such, the development and optimisation of agri-PV systems have garnered significant academic and industrial interest. This section explores the historical developments, a key performance metric, and the current trends in the optimisation of agri-PV systems.

2.1.1. Historical Development and Empirical Insights

The concept of agri-PV, which combines solar photovoltaic systems with agricultural practices, is designed to maximise land use by simultaneously generating sustainable electricity and agricultural outputs. The genesis of agri-PV can be traced back to a pioneering experiment at the Fraunhofer Institute in Germany (Goetzberger and Zastrow, 1981), where solar panels were installed about 2 m above crops. This setup was compatible with standard agricultural machinery and did not require extensive optimisation. This initial experiment set the stage for further exploratory projects, such as the first agrivoltaic pilot in France, which positioned mono-crystalline PV modules 4 m above the ground and demonstrated potential land productivity increases of 60 to 70% (Marrou et al., 2013). These early studies underscored the critical importance of thoughtful system design to balance solar panel density with sufficient light availability for the crops below.

Further research has continued to affirm the pivotal role of system design in the success of agri-PV systems. Studies have shown that well-planned agri-PV setups can boost land use efficiency, crop yields, and provide resilience against extreme weather conditions (Amaducci et al., 2018). For example, research suggests that optimal panel orientation and the ability to make dynamic adjustments are especially beneficial in arid areas, helping to moderate soil temperatures and reduce water evaporation (Valle et al., 2017, Trommsdorff, 2019). A significant empirical study in Almería, Spain, investigating the impact of various shading levels on lettuce crops, revealed that strategic shading could actually enhance agricultural productivity (Carreño-Ortega et al., 2021).

These foundational and ongoing studies demonstrate a complex relationship between solar energy production and agricultural productivity. They emphasise the vital importance of strategically placing and orienting PV modules to optimise agricultural yield, enhance land use efficiency, and protect crops from extreme weather. To effectively compare different layouts, it is crucial to define clear criteria and metrics to ensure they are evaluated on a uniform basis. One such important metric commonly used in literature is detailed in the following section.

2.1.2. Evolution of the Land Equivalent Ratio (LER)

The Land Equivalent Ratio (LER) emerged as a key metric within the agri-PV sector. It was initially introduced by (Mead and Willey, 1980) to evaluate the productivity of inter-cropping systems compared to mono-cultures as an indicator of land productivity. Expanding on this, (Dupraz et al., 2011) adapted the LER to evaluate systems that integrate multiple types of production such as agri-PV systems, see Figure 3.1, defining it through the equation:

$$LER = \frac{Y_{\text{cropAV}}}{Y_{\text{monocrop}}} + \frac{Y_{\text{electricityAV}}}{Y_{\text{electricityPV}}} \tag{2.1}$$

In Equation 2.1, "PV" represents a conventional PV plant, while "AV" denotes an agri-PV system. LER quantifies the efficiency of using land for dual purposes. A higher LER value suggests a more efficient system, capable of optimising the dual use of land for both agricultural and electrical production.

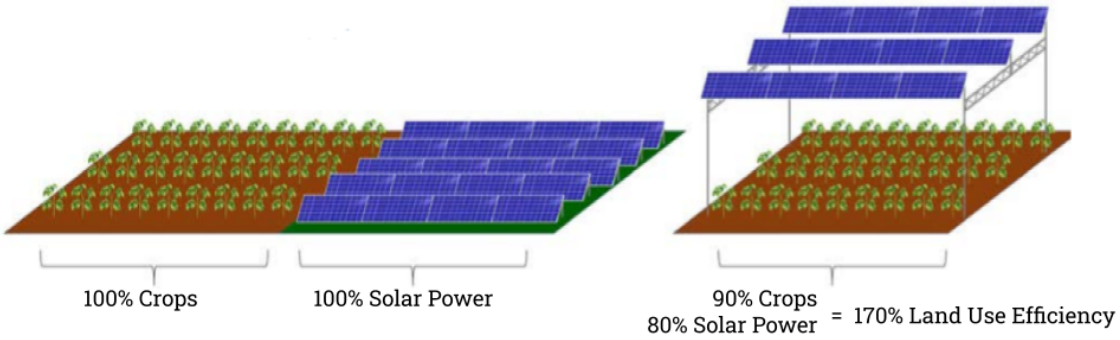

Figure 2.1: Land Equivalent Ratio (LER).

By doing a sensitivity analysis using LER, (Reasoner and Ghosh, 2022) explores the design variables that have the most impact on LER and thus which ones are necessary to optimise agri-PV systems. Notably, it highlights the importance of the tilt and azimuth angles of the PV modules (Kwon and Lee, 2021), as well as the spacing or density of the PV modules (Oleskewicz, 2020), (Sargentis et al., 2021), (Tahir and Zafar Butt, 2021), (Martín-Chivelet, 2016).

By strategically defining these system variables, one can significantly enhance LER. For instance, (Trommsdorff, 2019) underscores efficiencies of LER reaching 160% and 186% over two years in agri-PV systems by appropriately selecting the right solar panel density to control the shading projected onto the crops. Furthermore (Dupraz et al., 2011) also observed 135% to 173% efficiency of LER for the two densities of PV panels after three years of exploration.

This compelling evidence of success paves the way for further investigations into sophisticated modelling techniques that can simulate and optimise agri-PV interactions. Indeed, simulating such systems makes it easier to evaluate the impact of certain variables without the need of building a whole system and taking measurements over 2 year to have a sensible result. Recent advancements have seen (Trommsdorff et al., 2021) employing simulations and sensitivity analyses to evaluate the impact of design parameters on the solar radiation available to crops within agri-PV systems. Using LER, the study revealed potential

increase in land productivity ranging from 35% to 73% in scenarios utilising single and double tracking solar panels.

However, a critique by (Campana et al., 2021) argues that LER alone may not suffice for optimal agri-PV design. It advocates for the inclusion of additional objective functions to capture a more comprehensive view of the interaction between agricultural outputs and electricity generation. Indeed, LER compares two different quantities putting equal weights on PV and crops. This perspective warns that an excessive focus on maximising LER could compromise electricity production, impacting PV system investments, or potentially lead to crop failures. This critique emphasises the need for a broader optimisation framework that accommodates diverse priorities and outcomes, moving beyond the simple equivalence implied by traditional LER metrics.

2.1.3. Current Trends in Agri-PV System Optimisation

As the agri-PV sector progresses, the focus is expanding beyond merely maximising the Land Equivalent Ratio (LER) to encompass a broader spectrum of optimisation strategies. These strategies address the nuanced demands of simultaneous energy and food production, marking a crucial evolution from traditional methods to dynamic and complex models that accommodate diverse agricultural and photovoltaic efficiency metrics.

Innovators in the field are now leveraging advanced digital tools and multi-objective optimisation algorithms to redefine what it means to optimise agri-PV systems. For instance, a study by (Toyoda et al., 2023) showcases how design optimisation can vary significantly across different climatic conditions. By analysing agri-PV systems in varying climates, their work provides critical insights into how spatial configurations and panel orientations can be optimised to maximise both crop growth and solar energy production. This study emphasises the importance of considering local environmental conditions in the optimisation process, thereby enhancing the practicality and applicability of agri-PV designs.

Building on these insights, (Laue, 2022) introduces modelling techniques using ray tracing to simulate energy production and PAR levels in agri-PV greenhouses. Laue's models assess the influence of PV-array topologies and diffusive cover materials on light distribution within greenhouses. This approach not only predicts energy yield but also evaluates how well different greenhouse coverings can diffuse light to mitigate shadow effects from PV modules, crucial for optimising conditions for crop growth.

Furthermore, the research conducted by (Sumin and Sojung, 2023) introduces a sophisticated hybrid modelling approach designed to optimise the design of agri-photovoltaic systems under future climate scenarios in South Korea. Their framework combines environmental data with crop and solar energy simulations to predict and optimise the interactions between solar panels and crops under varying climatic conditions. This study highlights how adaptive agri-PV designs can significantly improve farm profitability and sustainability, especially in regions facing climatic changes, thus supporting a more climate-resilient agriculture.

Continuing this trend, (Mengi et al., 2023) introduces a pioneering method by developing a digital replica framework aimed at optimising based on crop-driven factors. This approach utilises digital simulations coupled with multi-objective genomic optimisation algorithms to effectively balance solar energy production with agricultural output. The model employs ray-tracing techniques to simulate sunlight distribution across the agrivoltaic system and explores various configurations. This exploration helps finding optimal setups that boost both energy yield and agricultural productivity. Importantly, the objective function of this model integrates critical parameters such as differences in ground absorbed energy, solar panel absorbed energy, crop yield, and water use efficiency between the agrivoltaic and traditional farming systems, which are weighted based on their importance as determined by the user. Meaning out of various functions, one objective function was formulated.

Despite the innovations, the method of assigning weights to different parameters and performance metrics is a subjective and complex task. This task demands a deep understanding of the trade-offs involved (M. T. M. Emmerich and Deutz, 2018), otherwise, it introduces a bias even before starting optimising the system. Moreover, it does not address the dependency issues associated with traditional LER metrics and faces difficulties in managing problems with complex Pareto fronts (Chahar and

Sharma, 2022).

Alternative optimisation strategies are being explored. (Campana et al., 2021) examines the use of strategically positioned, vertically mounted bifacial photovoltaic panels to maximise land use efficiency for concurrent food and electricity production. This study employs the NSGA-II algorithm, known for effectively optimising multiple objectives. While this research aims to improve LER, minimise power fluctuations to the grid, and boost annual electricity production, it is limited by the simplifications in the light model used to calculate shading areas, which may lead to conservative estimates of yield loss. Moreover, the reliance on LER within the objective functions introduces potential biases, emphasising the need for more sophisticated metrics in agrivoltaic system optimisation.

These developments underscore a dynamic shift towards more nuanced and multifaceted optimisation strategies in the agri-PV domain. From initial explorations to sophisticated digital frameworks, the field is evolving to address both the opportunities and challenges presented by integrating solar photovoltaic systems with agricultural practices. This evolution reflects a growing recognition that optimising for dual purposes requires moving beyond traditional metrics like LER to embrace a broader array of objectives that reflect the complex realities of modern agri-PV.

2.2. Multi-Objective Optimisation Algorithms

The complexity of agri-PV systems necessitates optimisation approaches capable of navigating the trade-offs between multiple conflicting objectives, such as maximising crop yield and optimising energy production. Multi-objective optimisation algorithms (MOOAs) provide a framework for finding solutions that effectively balance these competing goals. This section reviews several prominent MOOAs. Section 2.2.1 presents the theoretical foundations of multi-objective optimisation algorithms, Section 2.2.2 introduces evolutionary algorithms, Section 2.2.3 discusses particle swarm algorithms, and Section 2.2.4 introduces surrogate model-based algorithms. Finally, these algorithms are compared in Section 2.2.5 to determine which is best suited to meet the prerequisites of the simulations.

2.2.1. Theoretical Foundations of Multi-Objective Optimisation

The concept of multi-objective optimisation (MOO) dates back to the early works of (Edgeworth, 1881) and (Wicksteed, 1906), who introduced notions of optimal economic equilibrium and efficiency. Central to MOO is the Pareto Front or Pareto Optimal Set (Marler and Arora, 2004), which represents solutions that cannot be improved in one objective without worsening another. This concept was further developed by (Kuhn and Tucker, 1951), who established conditions for optimality in nonlinear programming.

Initially, multi-objective optimisation algorithms were adaptations of single-objective methods, tailored to handle multiple goals. An example is the Weighted Sum approach by (Zadeh, 1963), which aggregates multiple objectives into a single one by assigning different weights to each, according to their perceived importance. However, this method has several drawbacks, such as the subjective selection of weights, which may not always align with the preferences of the decision-maker, particularly in complex fields. It also struggles to identify solutions on non-convex portions of the Pareto front, thus potentially overlooking vital solutions (Audet et al., 2008). Moreover, as the number of objectives increases, the method becomes less scalable, complicating the weight adjustment needed to effectively explore the Pareto front.

The ϵ-Constraint method, introduced by (Marglin, 1967), is another approach that optimises one objective while treating the others as constraints. This method iteratively explores the trade-offs among objectives by varying the constraints. Despite its innovative approach, the method faces significant challenges, such as the critical selection of ϵ values which, if chosen incorrectly, can lead to an incomplete exploration of the Pareto front. This method also increases in computational complexity with the addition of more objectives and constraints, requiring the solution of separate optimisation problems for each ϵ setting. This can reduce its efficiency in large-scale applications.

2.2.2. Evolutionary Algorithms

Evolutionary algorithms (EAs) represent a significant leap forward in multi-objective optimisation (MOO), they first introduced by (Schwefel, 1965) in Germany. These population-based meta-heuristics emulate natural evolutionary processes and are now categorised into three types: dominance-based, indicator-based, and decomposition-based algorithms (Chahar and Sharma, 2022).

Dominance-Based Algorithms: Dominance-based algorithms assess fitness according to the principle of Pareto dominance, exemplified by techniques such as SPEA2 (Zitzler et al., 2001) and NSGA-II (Deb et al., 2002). However, in scenarios involving more than three objectives, these algorithms face challenges. The majority of solutions within the NSGA-II and SPEA2 frameworks become non-dominated, leading to a diminished search capability. For many-objective problems, the selection pressure decreases significantly as most individuals in the population do not dominate each other, which slows down the evolutionary process (Zhang and Xing, 2017).

Indicator-Based Algorithms: These algorithms utilise specific measures to rank or select individuals, bypassing the computational complexity involved in calculating Pareto dominance relationships. A popular measure used is the hyper-volume (S-metric) indicator, which helps guide optimisation algorithms toward effective Pareto fronts and assesses the quality of these fronts (Falcón-Cardona and Coello, 2019). For instance, the S-Metric Selection Evolutionary Multi-Objective Algorithm (SMS-EMOA) employs the hyper-volume indicator as its primary selection criterion and is optimised for smaller populations (Beume et al., 2006). However, the main drawback of these algorithms is the heavy computational load required to estimate indicators, which increases exponentially with the number of objectives and solution dimensions (Schutze et al., 2012).

Decomposition-Based Algorithms: These algorithms simplify the MOO problem by decomposing it into several smaller sub-problems, each optimised independently through scalarization techniques. This method leverages neighbourhood relationships, allowing solutions for adjacent sub-problems to benefit from each other's optimisations (Chahar and Sharma, 2022). An example is the Multi-Objective Evolutionary Algorithm based on Decomposition (MOEA/D) (Zhou et al., 2019). Despite its strengths, MOEA/D may struggle with non-uniform or highly complex Pareto fronts, performing best when the front is simple and evenly distributed (Cho et al., 2017).

Evolutionary algorithms, despite their proficiency in exploring diverse solutions, often suffer from slow convergence rates, especially in complex multi-objective contexts (Bechikh et al., 2017). This slow convergence becomes a significant issue in cases where function evaluations are costly or optimisation problems are dimensionally large. The efficiency of EAs also hinges on the precise setting of parameters such as population size, mutation rates, and crossover rates. Inappropriate parameter settings not only hinder efficient convergence but also increase computational demands, extending the time needed to reach viable solutions (Lavinas et al., 2021). This necessitates a delicate balance between exploration and exploitation to maintain diversity in the solution population while advancing towards optimal solutions.

2.2.3. Particle Swarm Algorithm

The Particle Swarm Optimisation (PSO) algorithm is inspired by the social behaviour patterns of organisms in swarms, such as birds flocking or fish schooling (Tang et al., 2021). This algorithm is employed to find optimal or near-optimal solutions to complex problems by navigating through a predefined set of parameters to maximise or minimise an objective function. It enhances solutions iteratively by improving the measure of quality associated with each candidate solution (Chahar and Sharma, 2022). In PSO, the trajectory of each particle (representing a potential solution) in the problem space is adjusted by blending the particle's own best-known position with the best positions discovered by the swarm, either globally or locally.

A specialised variant of PSO, the Multi-Objective Particle Swarm Optimisation (MOPSO), is designed to tackle multi-objective meta-heuristic challenges (Ahmed and Glasgow, 2012). MOPSO utilises a

repository or archive to retain non-dominated solutions, effectively representing the Pareto front. This method includes strategies to maintain diversity within the swarm, ensuring extensive coverage of the Pareto front (Coello, 2011). It is particularly effective for problems where the search space forms a graph that aids in identifying viable solutions.

While PSO and its variants like MOPSO are recognised for their simplicity and capacity to maintain diversity while converging towards robust solutions, they are not without limitations. These methods can experience slow convergence rates and are susceptible to becoming trapped in local optima if not carefully managed. Additionally, the effectiveness of these algorithms often hinges on the precise calibration of operational parameters such as swarm size and iteration count, which are critical for achieving optimal performance (Rajani et al., 2020).

2.2.4. Surrogate Model based Algorithm

As the complexity of real-world problems increases, researchers are continually seeking strategies to enhance computational efficiency and accuracy. Among these strategies surrogate modelling (Madsen et al., 2000) is a promising methodology for computationally intensive simulation, which is why these algorithms are further investigated in the following question.

Surrogate models are a pivotal tool in managing high computational demands. These models substitute exact objective functions with faster-to-evaluate approximations, effectively reducing the computational load. The primary challenge lies in balancing computational speed with the accuracy of the models, with numerous methods developed to navigate this trade-off (Jiang et al., 2019).

Surrogate problems are constructed by approximating each computationally expensive function using various meta-modelling techniques such as polynomial functions (Madsen et al., 2000), radial basis functions (RBFs) (Buhmann, 2000), Gaussian Processes models (Gramacy, 2020), and neural networks (Tipu et al., 2024). These approximations hinge on sample points selected from the decision space through diverse sampling techniques.

Surrogate-based methods are categorised into two main types based on how the surrogate models are updated: adaptive and sequential. These categories are developed from concepts found in prior studies (Queipo et al., 2005), (Wang and Shan, 2008), and (Kitayama et al., 2013). The Sequential Framework focuses on building an accurate surrogate model of the problem. This model is then used to approximate the Pareto frontier, which is the set of all non-dominated solutions. The goal is for this surrogate-derived Pareto frontier to closely match the true Pareto frontier of the original problem. The Adaptive Framework starts with an initial surrogate model that may be imperfect. This framework emphasises iterative updates and refinements to the model. Through this process, the approximated Pareto frontier is gradually adjusted to more closely reflect the true Pareto frontier of the original problem.

To refine the surrogate problem, new sample points are essential (Forrester et al., 2008). These points can be chosen from non-dominated solutions of the surrogate problem or from previously unexplored areas in the decision and/or objective space. This involves a critical balance between enhancing computational speed and maintaining model accuracy. The accuracy of the surrogate model is crucial in the sequential framework, as it must closely approximate the original problem's Pareto frontier (Jiang et al., 2019). A significant emphasis is also placed on evaluating and ensuring the surrogate model's accuracy using various statistical measures to avoid deviations from the original problem's objectives.

2.2.5. Comparative Analysis of Multi-Objective Optimisation Methods

The complexities of multi-objective optimisation (MOO) in agri-PV systems necessitate a meticulous evaluation of various optimisation methods to determine their suitability for this specific application. The optimisation algorithms available in the literature review are primarily based on irradiation models and objective functions that are noise-free and inexpensive to evaluate. In this study, a different modelling approach was selected and therefore a more suitable optimisation algorithm is necessary.

First and foremost, effective optimisation algorithms must adeptly handle black box functions, which are prevalent in systems utilising software like Radiance. Radiance's complex mathematical underpinnings,

including unknown properties such as convexity or continuity, often obscure the direct application of traditional optimisation techniques. Surrogate model-building algorithms and certain adaptive frameworks, as noted by (Laumanns and Ocenasek, 2002) and (Tabatabaei et al., 2015), excel in managing these functions by effectively addressing their complex properties.

Secondly, the inherent complexity of agri-PV systems often embodies conflicting objectives, such as balancing crop yield against energy production. It is essential that the chosen optimisation algorithm can adeptly manage these multiple objectives. Techniques such as NSGA-II and MOEA/D are particularly well-suited for this task, as they are designed to handle complex, multi-objective problems by efficiently balancing trade-offs (Chand and Wagner, 2015).

Thirdly, the optimisation process in this context involves computationally intensive tools, notably the use of Radiance software. Surrogate model-based methods are advantageous here, especially those employing adaptive frameworks that approximate expensive objective functions. This strategy significantly reduces computational loads, enabling quicker evaluations and iterative enhancements (Tabatabaei et al., 2015), thus enhancing overall efficiency.

Finally, the variability and unpredictability introduced by tools like Radiance demand methods that can effectively manage stochastic behaviours. Algorithms such as variants of Particle Swarm Optimisation (PSO) and adaptive surrogate-based methods are preferred for their robustness in dealing with stochastic elements. These methods ensure more accurate and reliable optimisation outcomes, as detailed by (Ahmed and Glasgow, 2012) and (Peter Frazier, 2018).

Based on the identified attributes, several insights guide the selection of optimal multi-objective optimisation methods for agri-PV research:

- Evolutionary Algorithms: These methods are robust in managing multiple objectives and constraints but may exhibit slow convergence speeds in complex scenarios. Their efficiency decreases with increased computational demands.
- Particle Swarm Algorithms: Effective in maintaining solution diversity, these methods can suffer from slow convergence and may become trapped in local optima without proper tuning.
- Surrogate Model based Algorithm: Excel in scenarios with high computational costs by using approximations to reduce the frequency of costly function evaluations, speeding up the optimisation process. However, their success heavily depends on the accuracy of the surrogate models.

Considering the specific challenges of agri-PV system optimisation, a surrogate model-based approach is recommended for the specific irradiation modelling approach selected. It offers a balanced solution to achieve computational efficiency, maintain solution diversity, and ensure accuracy, enhancing the decision-making process in multi-objective optimisation scenarios.

3

Methodology

This chapter details the methodology employed throughout the thesis research. Section 3.1 outlines the simulation framework of the model, by providing details and assumptions on the agri-PV system configuration, the irradiation modelling and optimisation problem. Section 3.2 defines the optimisation algorithm and its components for both single and multi-objective optimisations. Finally, Section 3.3 details the application of the proposed framework to a case study in an apple orchard in Northern Italy.

3.1. Simulation Framework

To remind the reader, the objective of this thesis is to develop an optimisation algorithm to optimise the layout of agri-PV systems. The corresponding global flowchart is presented in Figure 3.1, where the focus of this study is primarily on the optimisation algorithm.

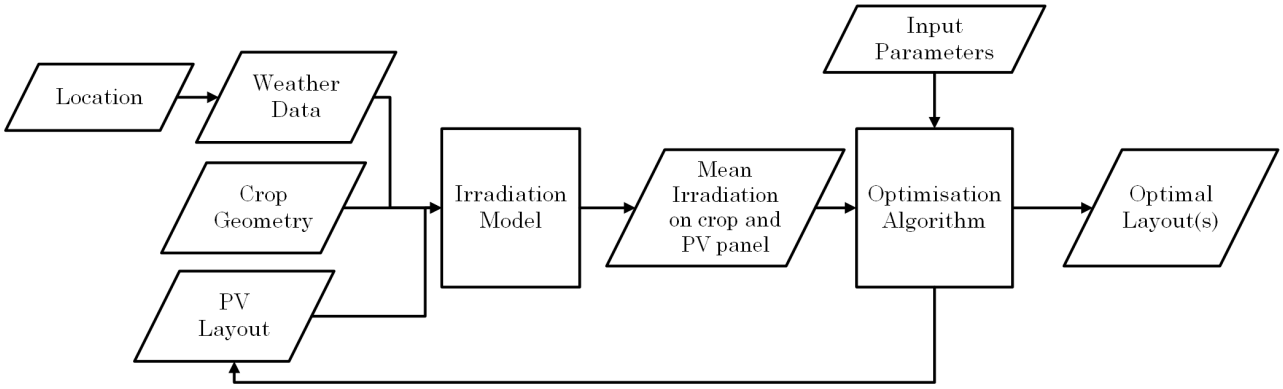

Figure 3.1: Agri-PV layout optimisation framework.

3.1.1. Agri-PV System Configuration

The field is assumed to be rectangular, with variable dimensions along the x and y axes. Additionally, the orientation of the field is adjustable. For the purposes of this model, the field is considered flat to simplify calculations, and the horizon is assumed to be open and unobstructed.

Regarding the PV components of the agri-PV system, the system utilises fixed, east-west facing bifacial solar panels. These panels can be oriented in either portrait or landscape modes. Variables such as hub height, pitch, and the number of stacked solar panels are adjustable to fit the specific requirements of the agri-PV system. Additional parameters including panel size, number of cells, and cell gap spacing are also modifiable. The system configuration allows changes in the number of strips and the length of

each strip.

The simulated crops are orchard trees, with adjustable characteristics such as tree size, pitch, strip length, and the number of strips. This flexibility allows for detailed customisation of the agricultural component of the agri-PV system.

3.1.2. Irradiation Modelling

Radiance simulations require specific inputs such as weather files that include data on Global Horizontal Irradiance (GHI), Direct Normal Irradiance (DNI), and Diffuse Horizontal Irradiance (DHI). These GHI files are sourced from EURAC's local weather stations and ensure the accuracy and relevance of the simulation's environmental conditions. From GHI, through a Perez all-weather sky model, the DNI and DHI values are deduced.

The software Radiance, employs the "gencumsky" approach to generate cumulative sky models, crucial for simulating day-lighting and solar radiation over extended periods. This method aggregates sky conditions over a specified period into a single representative model, enhancing computational efficiency and providing a robust basis for simulation (Robinson and Stone, 2004).

Irradiation values for the agri-PV system are derived from sensors strategically positioned across the crops, from top to bottom and on each side of the tree, as well as on both the front and rear sides of each PV panel, as depicted in Figure 3.2. Radiance employs backward ray-tracing techniques to calculate the colour, intensity, and distribution of light within the modelled environment, making it particularly effective for applications involving complex plant geometries and variable light conditions.

Figure 3.2: Agri-PV orchard consisting of multiple crop strips with the same pitch as the PV array.

Simulations for solar panels are conducted annually, calculating mean irradiation values in [Wh/m^2]. For the orchard, irradiation is computed only during the growing season. This method simplifies the analysis by focusing on average outcomes rather than hourly fluctuations and effectively reduces the duration of light simulations.

3.1.3. Optimisation Problem

The optimisation framework is designed to accommodate multiple objectives linked to system irradiation, with user-defined design variables such as tilt, pitch, hub height, and cell gap spacing.

The primary aim is to optimise the agri-PV system layout efficiently, avoiding the use of the Land Equivalent Ratio (LER) as a performance metric due to its identified limitations in the literature review in

Section 2.1.2. Consequently, the study adopts a dual-strategy approach: a multi-objective optimisation to mitigate the dependency on LER and a single-objective method for comparative performance analysis.

Although LER typically considers both crop yield and electricity yield, this study specifically focuses on radiation data, leveraging its availability through Radiance software. This decision is supported by the direct correlation between solar radiation and the output current of solar panels; increased solar radiation directly enhances solar panel performance (Attaviriyanupap et al., 2011). Similarly, crop yield is profoundly affected by Photosynthetically Active Radiation (PAR), which ranges from 400 nm to 700 nm (McCree, 1981)—a spectrum that Radiance is capable of accurately simulating. Thus, the objective function for the single-objective optimisation in this study is formulated based on these considerations.

$$\text{Max } F(t,f) = \text{Max } \frac{1}{N}\sum_{i=1}^{N} I_{crop,i} + \frac{1}{M}\left(\sum_{i=1}^{M} I_{front,i} + I_{back,i}\right) \tag{3.1}$$

Here, N and M respectively denote the number of sensors on the crop and on the PV panel. $I_{\text{crop},i}$ refers to the radiation measured by the i-th sensor on the crop, and $I_{\text{front},i}$ and $I_{\text{back},i}$ denote the radiations on the i-th sensor on the front and back sides of the PV panel, respectively.

For multi-objective optimisation, the objectives are separated into maximising the mean photosynthetic radiation (PAR) on the crops and mean radiation on the solar panels:

$$\text{Max } F_1 = \text{Max } \frac{1}{N}\sum_{i=1}^{N} I_{crop,i}, \qquad \text{Max } F_2 = \text{Max } \frac{1}{M}\left(\sum_{i=1}^{M} I_{front,i} + I_{back,i}\right) \tag{3.2}$$

This strategy ensures a balanced optimisation of radiation effects on both the crops and solar panels. The objective function uses radiation measured in kilowatt-hours [kWh]. This is calculated by multiplying the irradiation value, provided in kilowatt-hours per square meter [kWh/m^2] by Radiance, by the active area. The active area refers to the portion of a surface directly involved in interacting with sunlight. For crops, the active area is the part of the plant exposed to sunlight, which is critical for photosynthesis. For solar panels, the active area includes all sections containing photovoltaic cells that convert sunlight into electricity.

Design Variables and Constraints

The design variables of the optimisation algorithm specifically represent the degrees of freedom in the PV layout. As discussed in Section 3.1.1, these variables can encompass any aspects associated with the PV layout. While the model is initially designed to handle two variables, it is easily adaptable to accommodate three or more variables.

The system also handles a single constraint, ensuring that the shading from solar panels does not significantly reduce crop yield, crucial for maintaining the dual objectives of agricultural productivity and energy production (Elborg, 2017):

$$I_{APVcrop} \geq \alpha \cdot I_{FScrop} \tag{3.3}$$

Here, $I_{APVcrop}$ represents the mean PAR on crops within an agri-PV system, and I_{FScrop} denotes the mean PAR on crops under full sun conditions, i.e., without any solar panels. The factor α signifies the acceptable percentage reduction in crop yield due to the shading effect of the PV installation. This constraint not only safeguards agricultural output but also aligns with regulatory standards on the permissible reduction in land usability for agriculture due to PV installation, which varies by country (European Commission. Joint Research Centre., 2023).

3.2. Optimisation Algorithm

Based on the literature review in Section 2.2, it was decided to employ a surrogate model-based optimisation approach. This decision was made because Radiance is computationally intensive software, and thus the number of iterations must be kept to a minimum, requiring the most efficient optimisation algorithm possible. In Section 3.2.1, the surrogate model of the optimisation algorithm is selected.

Section 3.2.2 provides a framework for the Bayesian optimisation algorithm based on the Gaussian process surrogate model. Section 3.2.3 provides insights on the Gaussian Process model and Section 3.2.4 on the acquisition function selected for the optimisation algorithms.

3.2.1. Selection of Surrogate Model-Based Optimisation Algorithms

Surrogate model-based optimisation is an efficient approach in multi-objective optimisation, particularly when dealing with problems that involve expensive function evaluations. These methods involve creating simpler, computationally cheaper models that approximate the behaviour of the actual objective functions. Different types of predictive modelling techniques or machine learning algorithms were considered in order to choose the most suitable one for this study: Radial Basis Function (RBF) based Algorithms, Polynomial Regression (PR) Models, Neural Networks based Algorithms and finally Gaussian Process-based (GP) Algorithms. Note that each of these can be used within optimisation processes.

Radial Basis Function (RBF) use radially symmetric functions to model complex, multi-dimensional spaces, they are particularly popular in global optimisation algorithms to approximate unknown functions (Gutmann, 2001). Polynomial regression models establish relationships between variables using polynomial equations to then use the model to find the optimal point (Zhen-Yu and Yin-Fu, 2019). Neural networks, mimicking brain structure, consist of layers of interconnected nodes that activate based on certain thresholds to process data (Alizadeh et al., 2019). Gaussian process based algorithms provide a probabilistic approach to modelling the objective function, offering not only predictions but also an estimation of the uncertainty in those predictions, in order to make well-informed decisions about where to sample next in the search space (Boyle, 2007).

These four methods were compared using four criteria: complexity, efficiency, accuracy, and flexibility from problem-specific assumptions and data properties. These criteria were selected based on several considerations. Efficiency is critical due to the computationally intensive nature of the irradiance model. Accuracy is crucial because building a surrogate model requires that it be as precise as possible to ensure a sensible optimal result in the output. Finally, the optimisation system aims to be applicable to many agri-PV systems and easily adaptable in case of minor required changes at various stages of the optimisation process, hence the criteria concerning flexibility and complexity. The summary of this comparison is given in Table 3.1.

Based on the evaluation criteria outlined in Table 3.1, the Radial Basis Function (RBF) was not selected. Although it offers high accuracy, its complexity and dependency on the size of the input space reduce its suitability. Furthermore, RBF provides only moderate flexibility from problem-specific assumptions.

Polynomial Regression was also excluded. Despite its simplicity and reasonable accuracy, its efficiency diminishes as the polynomial degree increases, and it is particularly susceptible to noise—a significant concern due to the inherent noise in the Radiance software. Most critically, it requires precise specification of polynomial form and degree, making it less adaptable to the dynamic needs of our project.

Neural Networks, while potentially the most precise for modelling complex and non-linear systems, were not chosen due to their high complexity and lower efficiency. The considerable data requirements for effective training would likely be unfeasible within the scope of our study.

Ultimately, this evaluation leads us to conclude that Gaussian Processes (GP) are the optimal choice for our study, despite their inherent complexity. They strike a favourable balance between efficiency and accuracy and provide substantial flexibility from the functional form of the data. This flexibility is crucial for our optimisation needs, where the objectives are complex and the underlying phenomena are not well-characterised.

Upon establishing the surrogate model foundation for the agri-PV optimisation algorithm, the next critical step was selecting a specific algorithm suited to our needs. Among the various algorithms that utilise Gaussian Processes, ParEGO and Bayesian Optimisation are notably prominent. ParEGO effectively transforms multi-objective optimisation problems into single-objective challenges using a scalarization technique. It iteratively optimises this scalarized objective function, using the GP as a surrogate model. ParEGO employs random weights to scalarize multiple objectives, making it

Criteria/Model	Description
Complexity	
Radial Basis Function (RBF)	More complex than simple polynomial models.
Polynomial Regression (PR)	Variable complexity as uses polynomial equations, ranging from simple to highly complex based on the polynomial degree.
Neural Networks	The most complex, capable of modelling highly non-linear relationships, adjustable via network architecture.
Gaussian Process (GP)	Complex due to maintaining a probabilistic model of the Pareto front.
Efficiency	
Radial Basis Function (RBF)	Efficient with moderate-sized datasets but less so with larger input spaces.
Polynomial Regression (PR)	Highly efficient with small, simple datasets; efficiency decreases with polynomial degree and dataset size.
Neural Networks	Less efficient due to significant computational resources required for training but fast at making predictions once trained.
Gaussian Process (GP)	Highly efficient in scenarios where function evaluations are expensive.
Accuracy	
Radial Basis Function (RBF)	High accuracy in interpolation tasks when basis functions fit well.
Polynomial Regression (PR)	Accuracy varies with polynomial degree; risk of under-fitting or over-fitting.
Neural Networks	Highly accurate for complex systems with adequate data and tuning.
Gaussian Process (GP)	Generally provides high accuracy and uncertainty measures.
Flexibility	
Radial Basis Function (RBF)	Moderately independent; performance varies with the match of basis functions to data behaviour.
Polynomial Regression (PR)	Dependent on correct polynomial specification; sensitive to data nature.
Neural Networks	Adaptable to various data types with minimal assumptions about data form.
Gaussian Process (GP)	Independent of functional form, assumptions tied to function smoothness through kernel choice.

Table 3.1: Comparison of Surrogate Models in Optimisation

particularly suitable for problems with two to three objectives (Knowles, 2006).

Alternatively, Multi-Objective Bayesian Optimisation (MOBO) expands upon the principles of single-objective Bayesian optimisation to manage multiple objectives. This framework utilises GPs to model each objective and leverages sophisticated acquisition functions such as the expected hyper-volume improvement (Frazier, 2018). One of its significant strengths is its versatility, allowing adaptation to a broad array of problem types (Picheny, 2015). Given these advantages, MOBO was chosen as the algorithm for this study, with additional details on its implementation provided in the subsequent section.

3.2.2. Framework of Bayesian Single Objective Optimisation

Having selected Bayesian optimisation (BO) as the algorithm for this study, this section outlines its framework for both single and multi-objective optimisation. Bayesian optimisation was initially introduced for single-objective problems by (Kushner, 1964) and further enhanced by (Jones et al., 1998). Multi-objective extensions of Bayesian optimisation, such as MOBO (Multi-Objective Bayesian Optimisation), were developed to handle multiple competing objectives simultaneously, expanding its application significantly. Comprehensive reviews on Bayesian optimisation can be found in (Frazier, 2018) and (Shahriari et al., 2016).

The single-objective optimisation problem typically involves searching for the minimum of an unknown black-box function, a function for which no closed-form or derivative information is available, defined as $f : \mathbb{R}^d \to \mathbb{R}$:

$$\min_{x \in \mathbb{R}^d} f(x). \tag{3.4}$$

This algorithm is especially effective for optimisation within continuous domains where the dimension is less than 20 ($d \leq 20$), particularly when the objective function f lacks defined characteristics such as concavity or linearity and can accommodate stochastic noise in function evaluations (Frazier, 2018).

Multi-objective Bayesian optimisation (MOBO) extends the BO framework to handle several conflicting objectives by employing a vector-valued function $\mathbf{f} : \mathbb{R}^d \to \mathbb{R}^k$, where k is the number of objectives. This is formalised as:

$$\min_{x \in \mathbb{R}^d} \mathbf{f}(x). \tag{3.5}$$

The general workflow of Bayesian optimisation is illustrated in Figure 3.3. Bayesian optimisation begins with initial sampling of the design space, where initial points are chosen uniformly at random $(x_i)_{i=1}^t$. Iteratively, the Gaussian Process (GP) model refines its predictions about the objective functions using data gathered from these evaluations. At each iteration, the next point x^* is selected by optimising the acquisition function $\alpha(x)$, where $x^* = \arg\max_{x \in \mathbb{R}^d} \alpha(x)$. This function $\alpha(x)$ is strategically crafted to balance exploration of new possibilities with exploitation of known advantageous ones, considering all objectives collectively. After evaluating x^*, the process repeats until a predetermined stopping criterion is met (Peter Frazier, 2018). Overall, Bayesian optimisation is structured around two principal components: the statistical model, which in this case is a Gaussian Process used to model the objective function, see Section 3.2.3, and the acquisition function which determines the next sampling point, further details are given in Section 3.2.4.

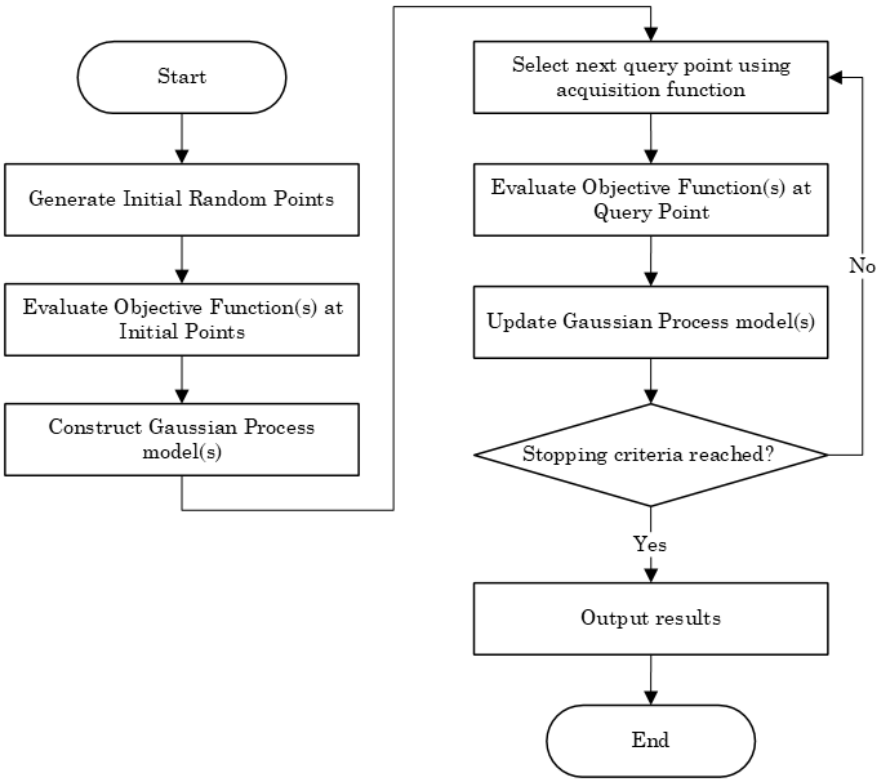

Figure 3.3: Agri-PV layout optimisation framework.

3.2.3. Gaussian Processes

Gaussian Processes excel in capturing and quantifying both uncertainty and the interplay between objectives. In the following, a brief introduction is given about Gaussian Process Regression in Bayesian approach, for a deeper overview, please refer to (Rasmussen and Williams, 2008).

Gaussian Process (GP) regression start by focusing on the objective function f and its values at a finite number of points, denoted as $x_1, \ldots, x_k \in \mathbb{R}^d$. For computational convenience, the function values at these designated points are grouped together into a single vector $[f(x_1), \ldots, f(x_k)]$. The vector of function values is considered an unknown quantity. Every unknown quantity is presumed to be drawn from some prior probability distribution. It is defined by a particular mean vector and a covariance matrix. The mean vector typically represents the expected values of the function at those points, while the covariance matrix encapsulates the expected relationships (correlations) between function values at different points. The entries of the covariance matrix are computed through a covariance function (or kernel) which depends on the points x_i and x_j and is parameterised by hyper-parameters θ. The kernel is chosen so that points x_i, x_j that are closer in the input space have a large positive correlation, encoding the belief that they should have more similar function values than points that are far apart. Resulting in the following prior distribution on $[f(x_1), \ldots, f(x_k)]$:

$$f(x_{1:k}) \sim \mathcal{N}(\mu_0(x_{1:k}), \Sigma_0(x_{1:k}, x_{1:k})), \tag{3.6}$$

where $x_{1:k}$ corresponds to $x_1, \ldots, x_k$, $f(x_{1:k}) = [f(x_1), \ldots, f(x_k)]$, $\mu_0(x_{1:k}) = [\mu_0(x_1), ..., \mu_0(x_k)]$ is a vector of the expected values of the function f at the points $x_1, ..., x_k$, and $\Sigma_0(x_{1:k}, x_{1:k})$ is a matrix that describes the covariance between the function values at different points in the input space, also called the kernel. The element $\Sigma_0(x_i, x_j)$, of the matrix represents the covariance between the function values at points x_1 and x_k.

In this case, the covariance matrix or kernel is defined using the Matérn kernel, which is robust to variations in data density and can model different types of smoothness in the data, even for higher-dimensional spaces (Melkumyan and Ramos, 2006). Matern kernels are characterised by a smoothness parameter ν which dictates the smoothness of the function. In this case $\nu = 5/2$ so that the kernel is suitable for modelling functions with some degree of smoothness but potentially abrupt changes (Rasmussen and Williams, 2008):

$$\Sigma_0(x_i, x_j) = \sigma^2 \left(1 + \frac{r}{\ell} + \frac{3r^2}{5\ell^2}\right) \exp\left(-\frac{r}{\ell}\right) \tag{3.7}$$

where $r = ||x_i - x_j||$ is the euclidean distance between the points x and x', σ^2 is the variance parameter and l is the length scale parameter, which controls how quickly the correlation between points decreases with distance. The mean of the data $\mu_0(x)$ is calculated using the observations in the dataset. This empirical mean is used to initialise the mean function of the GP model. This approach is practical for ensuring that the predictions of the Gaussian process are centred around the observed data, improving the accuracy of the model and convergence behaviour.

Now that the model is constructed, to deduce the value of $f(x)$ at a new point x, it is first established that $n = k + 1$ and $x_n = x$. Consider the vector $[f(x_{1:k}), f(x)]$ where $f(x_{1:k})$ is defined by Equation 3.6. The value of $f(x)$ is determined by the following conditional distribution, known as the posterior probability distribution, obtained by applying Bayesian rules (Rasmussen and Williams, 2008):

$$f(x) \mid f(x_{1:k}) \sim \mathcal{N}(\mu_k(x), \sigma_k^2(x)) \tag{3.8}$$

where the posterior mean $\mu_k(x)$ and the posterior variance $\sigma_k^2(x)$ are defined as:

$$\mu_k(x) = \Sigma_0(x, x_{1:k})\Sigma_0(x_{1:k}, x_{1:k})^{-1}(f(x_{1:k}) - \mu_0(x_{1:k})) + \mu_0(x) \tag{3.9}$$

$$\sigma_k^2(x) = \Sigma_0(x, x) - \Sigma_0(x, x_{1:k})\Sigma_0(x_{1:k}, x_{1:k})^{-1}\Sigma_0(x_{1:k}, x) \tag{3.10}$$

The mean of the distribution $\mu_k(x)$ represents the best guess of the value of the function at point x and is determined by computing a weighted sum of the deviations of observed data from their expected values

under the prior, adjusted by the expected relationship between the observed points and the new point $f(x_{1:k}) - \mu_0(x_{1:k})$, plus the prior mean at the new point $\mu_0(x)$. The posterior variance $\sigma_k^2(x)$ is equal to the prior covariance $\Sigma_0(x, x)$ less a term that corresponds to the variance removed by observing $f(x_{1:k})$

Note that the conditional distribution of f(x) can also be calculated at more than one unevaluated point by having a mean vector and covariance kernel that depend on the unevaluated points, the locations of the measured points $x_{1:k}$ and their measured values $f(x_{1:k})$.

To accommodate multiple objectives within Bayesian optimisation, a vector-valued GP is utilised. Each component of the vector represents a different objective, and the GP models them simultaneously, maintaining a covariance structure that captures interactions between the objectives. This setup facilitates the computation of acquisition functions that inherently consider multiple objectives, enabling a more coordinated exploration of the search space.

3.2.4. Acquisition functions

Acquisition functions are mathematical tools used in Bayesian optimisation to guide the search process for optimising an objective function. Their primary role is to decide the next point to evaluate by trading off between exploring uncharted areas of the design space and exploiting the areas known to yield good results. This balance between exploration and exploitation is crucial as it directly impacts the efficiency and effectiveness of the optimisation process. In practice, acquisition functions provide a scalar value for each candidate point in the search space, indicating the potential utility of evaluating the objective function at that point. A higher value suggests a higher priority for sampling at that point, guiding the optimisation algorithm towards the most promising areas under the current uncertainty of the model.

Single Objective Optimisation:
In single-objective Bayesian optimisation, common acquisition functions include Probability of Improvement (PI) and Expected Improvement (EI). PI is the simplest and one of the earliest acquisition functions, which quantifies the probability that a given point will improve over the best current observation. It tends to be more exploitative, especially in regions close to the current best (Kushner, 1964). EI quantifies anticipated improvements at each point in the input space over the best observed value, based on predictive distributions from a Gaussian Process. This metric effectively guides the next sampling location by estimating where significant improvements are most likely, based on the current model. It balances exploration and exploitation by favouring regions where the model predicts significant improvements with a reasonable degree of uncertainty (Mockus, 1974). Mathematically, it is expressed as:

$$EI(x) = \mathbb{E}\left[\max(f(x) - f(x^*), 0)\right] \tag{3.11}$$

where $f(x^*)$ is the best observed objective value so far (Frean and Boyle, 2008). EI (Expected Improvement) is often chosen for global optimisation tasks because it effectively balances exploration and exploitation based on the expected magnitude of improvement. This makes EI particularly well-suited for complex optimisation challenges where the landscape of the objective function is poorly understood or highly irregular. Empirical studies and practical implementations have frequently demonstrated that EI tends to outperform PI (Probability of Improvement), especially in scenarios where function evaluations are costly or the search space is vast and complex (Snoek et al., 2012). Therefore, EI is employed for the single-objective optimisation in this study.

Multi Objective Optimisation:
The Expected Hyper-volume Improvement (EHVI) extends the single-objective Expected Improvement (EI) metric to accommodate multiple, often conflicting objectives through Gaussian Process (GP) models. In the multi-objective optimisation context, the EHVI is particularly valuable as it calculates the expected increase in the dominated volume, which is the space between the current Pareto front and a potential new Pareto front resulting from the inclusion of a new point (M. Emmerich et al., 2006). This process emphasises balanced improvements across the objectives without inherently favouring one over another.

The hyper-volume measure, a common metric used to determine the quality of a set of solutions to a multi-objective optimisation problem, is defined as the Lebesgue measure of the hyper-volume covered by the boxes that have an element of a set P as their upper corner and a user-defined reference point r

as their lower corner. Here, P represents a set of currently non-dominated points in the objective space, part of the Pareto front approximation. The reference point r must be dominated by all points in P, ideally by all points of the Pareto front as well (M. Emmerich et al., 2006).

$$\text{EHVI}(P) = \int_{\mathbb{R}^m} HI(p, P) \times PDF(p)\, dp$$

where $HI(p, P)$ represents the hyper-volume improvement and $PDF(p)$ is the probability distribution function over points in the objective space. The EHVI calculation utilises two specific functions, Psi and Nu to compute the incremental hyper-volume contributions for intervals in the objective space (Hupkens et al., 2014):

$$\Psi(a, b, \mu, \sigma) = \sigma \cdot \phi\left(\frac{b-\mu}{\sigma}\right) + (b-a) \cdot \left(1 - \Phi\left(\frac{b-\mu}{\sigma}\right)\right) \tag{3.12}$$

$$\nu(lb, ub, \mu, \sigma) = (ub - lb) \cdot \left(1 - \Phi\left(\frac{ub-\mu}{\sigma}\right)\right) \tag{3.13}$$

- a and b are the lower and upper bound of integration (often the current Pareto front boundary).
- lb and ub are the lower and upper bounds of the segment considered for hyper-volume contribution.
- μ and σ are the mean and standard deviation, respectively, of the Gaussian Process (GP)'s predictions at the point being evaluated.
- ϕ and Φ represent the probability density function (PDF) and cumulative distribution function (CDF) of the standard normal distribution, respectively.

In the application of EHVI, these functions are calculated for each point and combined to form the overall EHVI across all cells and objectives. This detailed computational framework supports the advanced management of multiple objectives, facilitating a more coordinated exploration of the search space.

3.2.5. Implementation of Bayesian Optimisation

In order to guarantee easy usage by the user, the optimisation process requires minimal input as only three key parameters are required. The first is the number of initial data points, which are sampled to initialise the Gaussian Process model, generally between 2 to 10. The second is the exploration factor for the acquisition function; this parameter determines the balance between exploitation and exploration that the acquisition function should choose. A high exploration number means that the algorithm samples query points more scattered throughout the design space. Finally, the maximum number of iterations is required in case no other stopping criteria are met, ensuring the optimisation concludes after a finite number of loops.

Regarding the stopping criteria, the optimisation loop ends based on three specific conditions. The first is the total iteration count, which is a required input. Secondly, if no improvement in the optimal solution has been observed after a set number of iterations (usually 10), the optimisation loop is stopped. Finally, if a certain precision level in the surrogate model (usually 95% accuracy) is reached by the GP model, the optimisation loop is also terminated.

3.3. Case Study: Apple Orchard Field in northern Italy

In the following section, details of the creation and analysis of a digital replica of the agri-PV system considered in the case study are given. Section 3.3.1 provides a detailed overview of the field setup and layout, Section 3.3.2 offers specific information about the variables and sensor placement used in the study, and finally, Section 3.3.3 presents the comparison between classical Radiance simulations and the surrogate models used for optimisation.

3.3.1. Field Description

This section provides a detailed overview of the agri-PV system simulation conducted in an apple tree orchard located in northern Italy. The simulation settings are visualised in Figure 3.4, which illustrates the layout of the agri-PV system.

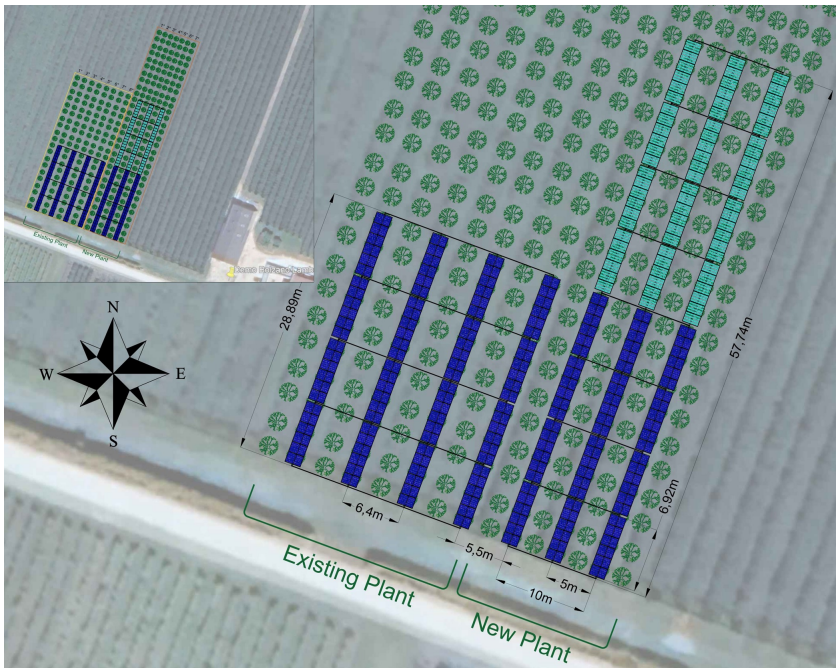

Figure 3.4: Field and agri-PV system layout.

The study is confined to the New Plant (NP) part, depicted in a dark shade of blue in the figure, excluding the light blue areas that are not taken into account in the surrounding of the studied agri-PV system. The Existing Plant (EP), however, is included and remains unchanged throughout the study. The configurations of the EP consists of eight rows of orchards and photovoltaic panels, with a pitch of 3.2 m. The solar panels are mounted at a hub height of 4.5 m and are set at a tilt angle of 15 °. The field is oriented 20.3 ° east.

The New Plant system occupies a field measuring 30 m by 17.5 m and the same orientation. It features bifacial solar panels sized 1.1 m x 1.7 m with 144 cells arranged in a 6x24 configuration in portrait mode. These panels are not stacked but are installed in fixed positions, aligning with the orchards at a pitch of 3.5 m and facing east-west. There are a total of seven rows. The panels, made of translucent glass from the brand Aleo, are mounted at a hub height of 4.5 m, while the orchard trees reach up to 3.5 m in height, ensuring sufficient light penetration and machinery passage.

This layout is designed to efficiently integrate solar energy production with agricultural operations, highlighting the potential benefits and configurations of agri-PV systems in enhancing the sustainability of agricultural practices.

3.3.2. System Specificities

This study involves the creation of a digital replica of an agri-PV system. The focal point of this digital model is at the centre of the New Plant (NP) field, specifically on the fourth row and twelfth solar panel. To comprehensively gather data on radiation across various surfaces—including both sides of the PV panel and the entire orchard—sensors are meticulously placed. Each PV panel is equipped with sensors equal to the number of cells along the y-axis, typically 24, on both the front and back sides. The orchard trees each host 63 sensors: 31 on the east side, 31 on the west, and one at the top, ensuring detailed coverage.

Radiance software simulates radiation, calculating mean values over a year for each sensor on the solar panels and orchard trees. While radiation data for the solar panels is collected year-round, the crop's Photosynthetically Active Radiation (PAR) is specifically monitored during the growing season from March to September. Outside the growing season, from October to February, the orchard's tree geometry, which lacks leaves, is not taken into the PV panel radiation calculations.

The optimisation considers tilt and cell gap distance as primary variables, influenced by their significant impact on PV power generation and sun hours on the farm land, respectively (Kuo et al., 2023). Contrary to (Kuo et al., 2023), the model of this study maintains a constant PV panel size, even as cell gap distance increases, requiring the removal of a cell line at certain thresholds to keep the panel size uniform, which could reduce overall electricity production.

Tilt angles vary from -90 degrees for east-facing to +90 degrees for west-facing orientations, with a neutral position at 0 degrees laying the panels horizontally. The cell gap factor, adjustable from 1 to 13, dictates the spacing between cells, impacting both light interception and panel efficiency (Figure 3.5). At the maximum setting, the gap equals the cell size, necessitating the removal of cell lines to preserve panel size and potentially affecting power output.

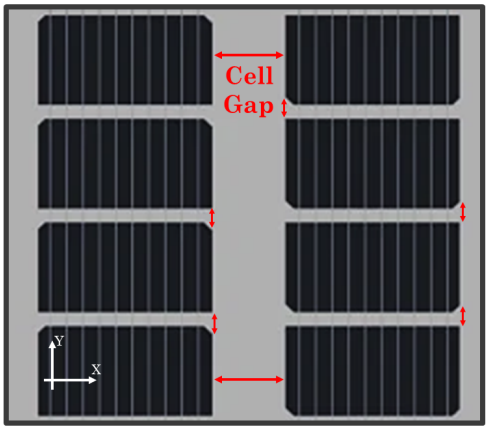

Figure 3.5: Cell gap between solar cells on a PV panel representation.

3.3.3. Classical Radiance

In order to asses the results of the optimisation algorithm for both single and multi-objective, their surrogate models are compared to classical Radiance data. To obtain classical Radiance data, a total of 598 agri-PV layouts are evaluated using the software, with a total simulation time extending over four days. The results are visually represented in Figure 3.6, where each square corresponds to a specific radiation level, with the corresponding tilt and cell gap factors at the centre of each square.

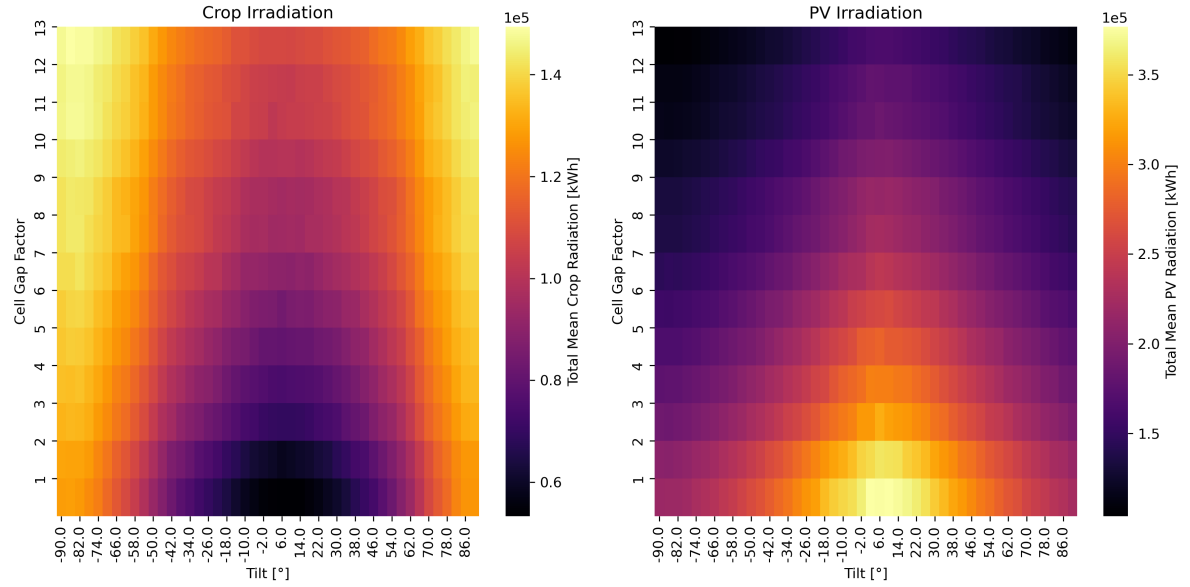

Figure 3.6: PV and Crop Radiation evaluated using Radiance.

Subsequently, these empirical results are compared in Section 4 against predictions made by the surrogate model. Although not every possible configuration is explicitly evaluated during the optimisation process, Gaussian Process (GP) models leverage gathered data to predict outcomes across the entire design space. This predictive capability allows the surrogate model to estimate radiation values for the same configurations assessed in the Radiance software.

The comparison between the empirical data maps and the surrogate model predictions involves the Mean Absolute Error (MAE). MAE measures the average magnitude of errors in the predictions, and accuracy is subsequently defined as:

$$\text{Accuracy} = 1 - \frac{\text{MAE}}{Max(\text{Error})}, \tag{3.14}$$

where MAE is normalised by dividing it by the maximum observed error in either dataset. This metric quantifies how well the model's predictions align with the actual observed data. A lower MAE indicates that the model's predictions closely match the observed values, denoting higher precision and reliability, thus reflecting higher accuracy.

4

Comparison of Gaussian Process Model with Classical Radiance

This master thesis focuses on utilising optimisation algorithms to determine the optimal layout for agri-PV systems. Based on a literature review in Section 2, it was decided to employ a surrogate-based algorithm. Therefore, assessing the accuracy of such a model is crucial. This section is dedicated to validating the surrogate model for single and multi objective optimisation in Section 4.1 and 4.2, respectively. The accuracy of the GP model is assessed after 80 iterations for each type of optimisation. As outlined in Section 3.3.3, then the predictive values generated by the GP model are compared with the results from Radiance simulations.

Following the model validation, a sensitivity analysis for both single and multi-objective optimisation is conducted in Section 4.1.2 and 4.2.2. It examines the impact of various input settings on the optimisation algorithms. Different combinations of initial sample sizes (ranging from 2 to 10) and exploration factors (categorised as low, medium, and high) are tested. For each scenario, the optimisation loops are executed under these varied settings to observe their influence on the model's performance.

The sensitivity analysis involves two runs for each optimisation algorithm. In the first run, trials continue until the model achieves or exceeds a mean 95% accuracy threshold, with the required number of iterations recorded. In the second run, a fixed number of objective function evaluations is set at 30. This means that if the initial sample size is 10, the optimisation algorithm will conduct 20 iterations; if the initial sample size is 2, then the number of iterations will be 28. Finally, the accuracy of each GP model is evaluated at the end of the defined number of iterations. This comprehensive analysis aids in understanding the model's sensitivity to initial conditions and parameter settings, ensuring robustness and reliability in its predictive capabilities.

4.1. Single Objective Optimisation

In this section the Gaussian Process model of the single objective optimisation algorithm is assessed in Section 4.1.1, followed by a sensitivity analysis in Section 4.1.2.

4.1.1. Assessment of Accuracy

After conducting 80 iterations with 10 initial samples and a low exploration factor, the results are visualised in Figure 4.1. Both graph represent the colour map of the single objective function corresponding to the sum of crop and PV radiation. The left graph displays the objective function computed by Radiance, representing exact values for each square whereas the right graph illustrates the same points predicted by the GP model. The distribution of accuracy across the same design space is shown in Figure 4.2.

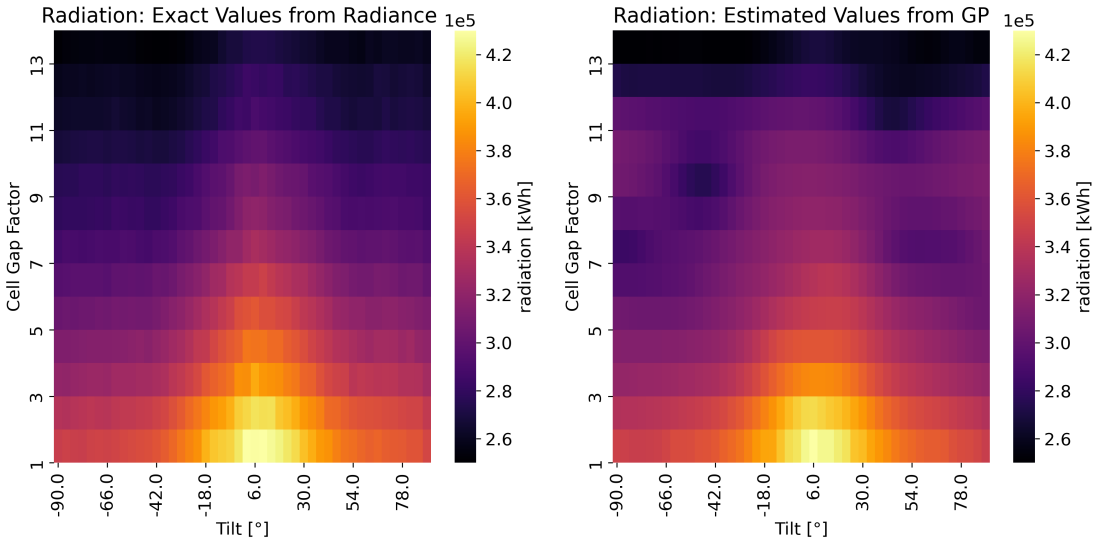

Figure 4.1: Comparison of the design space for the sum of crop and PV mean radiation with tilt and cell gap spacing as variables, for 80 iteration in single objective optimisation algorithm.Mean accuracy is (98.1 ± 1.7)%

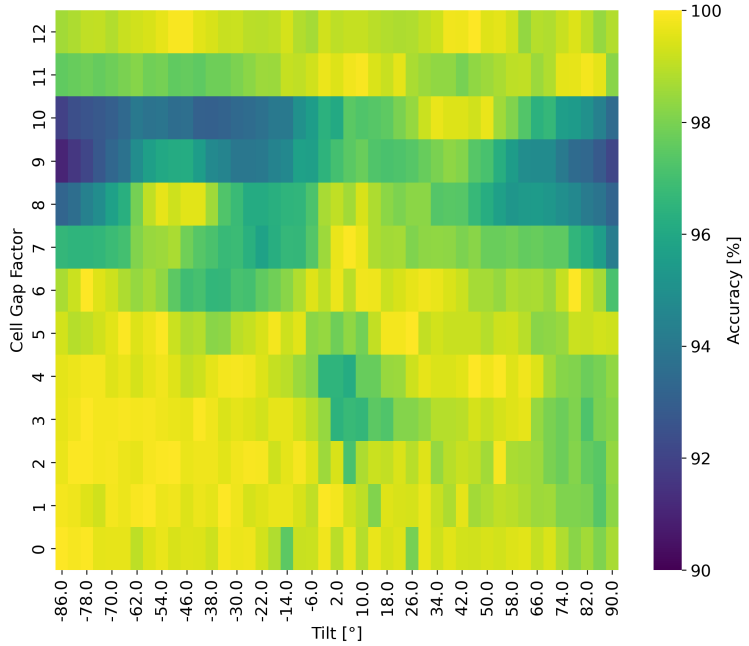

Figure 4.2: Objective function accuracy compared to classical Radiance values across the design space for single objective optimisation.

The mean accuracy of the proxy objective function after 80 iterations stands at 98.1% with a standard deviation of 1.7%. Considering this mean accuracy and observing Figure 4.1, it is evident that the Radiance simulations, requiring over four days to complete, contrast with the results from the GP model, which were obtained in less than ten hours and achieved an impressive 98.1% accuracy. Additionally, the standard deviation of 1.7% is relatively low and indicates satisfactory consistency. The comparison of the two graphs in Figure 4.1, the overall gradient on the colour map is similar, although the area showing maximum radiation appears smaller in the GP model. The GP model graph exhibits some

darker shades in the top right and left sides, likely due to a lack of query points in these areas. This observation is highlighted in Figure 4.2, where in the same region the accuracy is smaller. This suggests that caution should be exercised when using specific, isolated values instead of considering the entire spectrum. Generally, the GP model effectively captures the general trends within the design space.

The analysis from a practical perspective of the trends in Figure 4.1 reveals insightful trends. Moderate tilt angles and a small to medium cell gap factor generally yield the highest total radiation values, offering a balanced approach to maximising energy capture and allowing sufficient light for crop growth underneath the panels. The agri-PV field's slight eastward tilt of 20.3 degrees, as discussed in Section 3.3, appears to have a negligible impact on the radiation outcomes. The near symmetry of the data with respect to the zero on the x-axis confirms that this tilt does not significantly influence the results, underscoring the robustness of the model's predictions.

The evolution of this mean accuracy per iteration is depicted in Figure 4.3. The Figure shows a significant increase in accuracy within the first three iterations, followed by a slight decline. Another notable decrease in accuracy is observed after the 70th iteration, after which the model fails to recover to earlier accuracy levels by the end of the optimisation loop. This decrease may be attributed to the GP model incorporating new query points that diverge substantially from earlier data, potentially destabilising the model's predictions. Indeed, the hyper-parameters of the GP model are recalculated at each iteration, causing notable shifts in model behaviour based on newly evaluated data. Such re-calibration is part of the model's adaptive process to better fit the evolving dataset, although it can lead to temporary decreases in prediction accuracy if the new data is particularly challenging. Recovery from such disruptions can vary, in some cases, it may require numerous new evaluations to stabilise the model's accuracy. These findings underscore the potential benefits of terminating the optimisation process earlier in certain scenarios, for instance, when a predefined accuracy criterion is met.

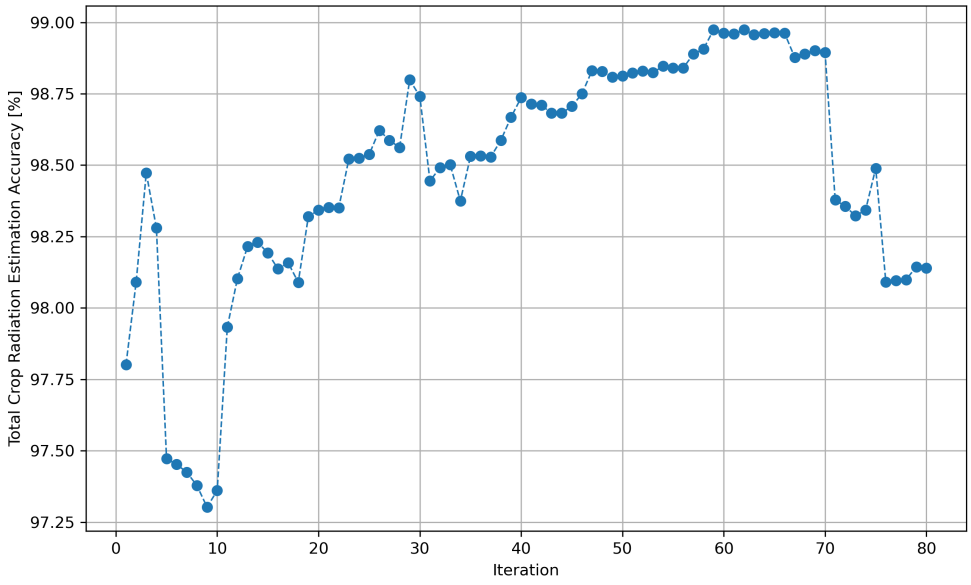

Figure 4.3: Accuracy of the objective function per iteration in single objective optimisation.

4.1.2. Sensitivity Analysis

A sensitivity analysis was conducted to evaluate the impact of input parameters on the performance of the single objective optimisation algorithm. This involved varying the number of initial samples and exploration levels. The required number of iterations to achieve at least a 95% accuracy for the GP model approximating the objective function was recorded, and shown in Table 4.1.

Exploration Level	2 Initial Samples	5 Initial Samples	10 Initial Samples
Low	25	12	1
Medium	4	2	1
High	5	5	1

Table 4.1: Number of iterations necessary to reach a 95% GP model accuracy for different levels of exploration and initial samples, for single objective optimisation.

In Table 4.1 the number of iterations required to reach 95% accuracy of the objective function decreases significantly as the number of initial samples increases. For example, when using a low exploration level, the required iterations drop from 25 with 2 initial samples to just 1 with 10 initial samples. This trend suggests that a larger pool of initial data allows the model to start closer to the optimal region, thereby reducing the number of iterations needed for convergence. Furthermore, higher initial samples tend to stabilise the performance across different exploration levels, indicating that having a robust initial dataset can compensate for less aggressive exploration strategies. Regarding the exploration levels, a higher exploration levels tend to show less variation in the number of iterations needed across different initial sample settings. Notably, with 10 initial samples, all exploration levels converge to a single iteration to reach 95% accuracy. This suggests that when enough initial data is provided, increasing the exploration does not necessarily translate into a higher computational burden in terms of iterations.

Additionally, to further analyse sensitivity, the total number of function evaluations was fixed at 30 to compare the final GP model accuracy across different settings. The accuracy for different exploration levels and initial samples are presented in Table 4.2.

Exploration Level	2 Initial Samples	5 Initial Samples	10 Initial Samples
Low	(96.0 ± 3.2)%	(96.5 ± 2.5)%	(96.4 ± 3.1)%
Medium	(99.1 ± 0.5)%	(99.0 ± 0.5)%	(99.1 ± 0.5)%
High	(99.0 ± 0.4)%	(98.9 ± 0.4)%	(99.1 ± 0.4)%

Table 4.2: GP model accuracy with standard deviation for different levels of exploration and initial samples, for single objective optimisation.

Table 4.2 shows high accuracy achieved across various settings, often exceeding 98%, which underlines the model's capability to reliably predict outcomes close to the true values modelled by Radiance simulations. Medium to high exploration consistently yields high accuracy (over 99%) and lower standard deviations, indicating that a higher exploration approach does not compromise accuracy and, in fact, enhances consistency across the design space. The lower standard deviations associated with medium and high exploration levels, especially with adequate initial samples, suggest that these settings offer a more reliable model output by minimising variability in performance.

The accuracy variation across the model's design space for different exploration levels is shown in Figure 4.4. Lower exploration factors result in more significant discrepancies in accuracy across the design space. Conversely, higher exploration factors lead to more uniform accuracy, thus mitigating results with fewer iterations.

In practice, this analysis would guide users to opt for a higher number of initial samples combined with medium exploration to ensure both high accuracy and low variability in outcomes. This strategy is particularly beneficial in reducing the computational load while still maintaining high model fidelity, making it an optimal approach for practical applications.

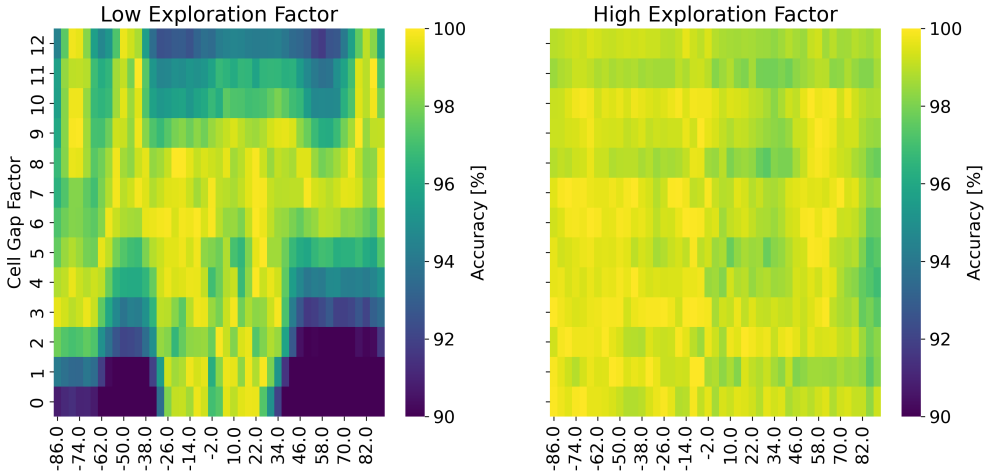

Figure 4.4: Objective function accuracy compared to classical Radiance values across the design space for low and high exploration factors in single objective optimisation.

4.1.3. Concluding Remarks

The results indicate that with appropriate input parameters, the process can be shortened significantly compared to using only classical Radiance, requiring as little as one hour to achieve 95% accuracy or higher instead of over four days. This efficiency is highlighted by the minimum of six objective function evaluations for medium exploration factor and 2 initial samples, as shown in Table 4.1. Furthermore, even in the worst-case scenario, the number of required evaluations does not exceed 27. Additionally, Table 4.2 shows that accuracy exceeding 98.1% is attainable with just 30 objective function evaluations, further demonstrating the potential for high accuracy within a few hours.

4.2. Multi-Objective Optimisation

In this section the Gaussian Process model of the multi-objective optimisation algorithm is assessed in Section 4.2.1, followed by a sensitivity analysis in Section 4.2.2.

4.2.1. Assessment of Accuracy

The multi-objective optimisation was conducted over 80 iterations with 10 initial samples and a low exploration factor. The optimisation loop was completed in less than ten hours which is significantly faster than the four days required by Radiance simulations. The GP model after the completion of the optimisation, had an accuracy for both objective functions of (98.2 ± 0.9)% for Crop PAR and (98.9 ± 0.8)% for PV module radiation.

Figures 4.5 and 4.6 provide a visual comparison between the exact radiation values from Radiance and the predictions from the GP model. In Figure 4.5, the left graph displays the exact crop PAR values computed by Radiance, serving as a benchmark, whereas the right graph shows the GP model's predictions. The close alignment of these two graphs indicates the model's high accuracy in predicting crop PAR across the design space. Similarly, in Figure 4.6, the left graph presents the exact radiation values for PV modules from Radiance, while the right graph illustrates the GP model's predictions.

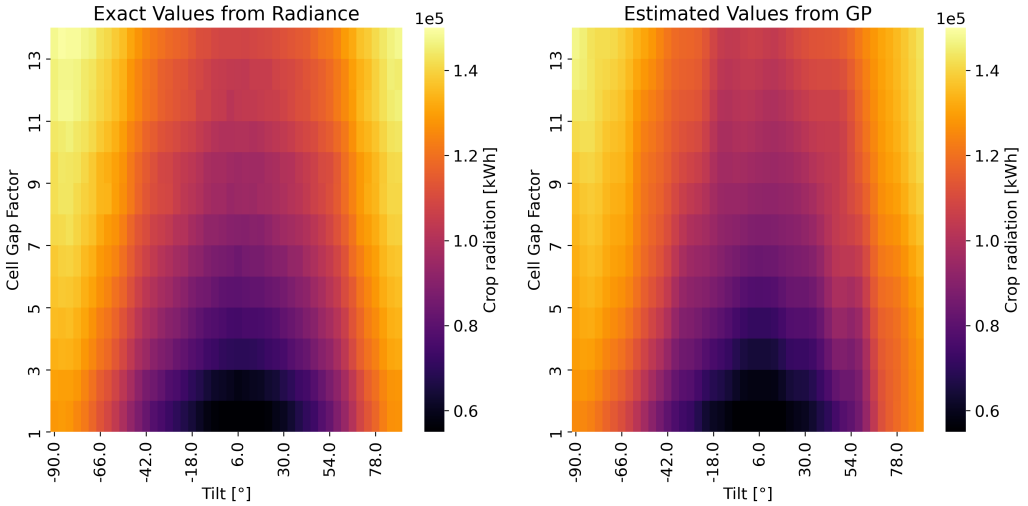

Figure 4.5: Comparison of the design space for the crop PAR with tilt and cell gap spacing as variables, for 80 iteration in multi-objective optimisation algorithm. Mean accuracy of (98.2 ± 0.9)%.

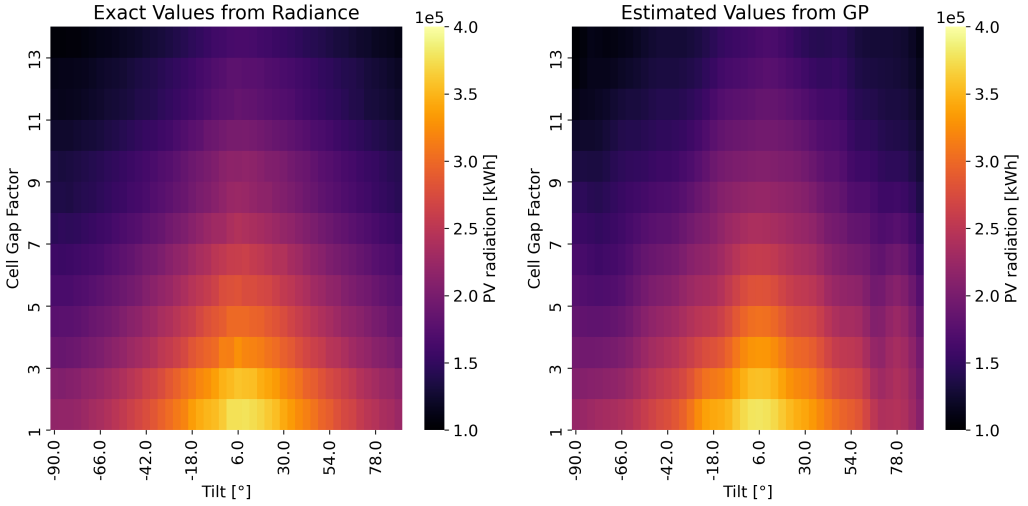

Figure 4.6: Comparison of the design space for the PV radiation with tilt and cell gap spacing as variables, for 80 iteration in multi-objective optimisation algorithm. Mean accuracy of (98.9 ± 0.8)%.

The analysis of Figure 4.5 reveals that the tilt angle appears to be the most influential variable for crop radiation. The radiation on the crop is minimised when the tilt angle of the solar panels is close to 0 degrees, meaning that the modules are horizontal. This effect can be mitigated by increasing the cell gap factor. A higher cell gap factor allows more radiation to reach the crops. On the other hand, the crop radiation reaches a maximum when the tilt angles approach -90 and 90 degrees, where the solar panels are vertical when minimal shadow is projected on the crops. Finally, the colour map seems to be slightly off-centred from the 0-degree tilt, angles facing west seams to be favourable. This is due to the fact that the field is located close to a mountain on its east side, which tends to block light coming from that direction. Note that the bifacial factor is not taken into account in this study.

Regarding PV radiation, Figure 4.6, the cell gap factor appears to be the most influential variable. Higher cell gap factors drastically reduce radiation on the PV panels as the active surface area of a module decreases (fewer solar cells per panel since the size of the solar panel remains constant). As for the tilt of the module, it is clear that tilt angles close to 10 degrees are optimal, with radiation decreasing as the tilt angle increases toward a more vertical position. Note that a similar off-centred symmetry is

also visible in the PV radiation colour map, confirming the hypothesis of it being caused by an external factor impacting the whole system.

The distribution of accuracy across the design space for both Crop PAR and PV module radiation is illustrated in Figure 4.7. The figure shows that the accuracy is uniformly high across the entire design space, with minimal deviations. This uniformity suggests that the model's predictions are not only accurate but also evenly reliable across different configurations of tilt angles and cell gap factors.

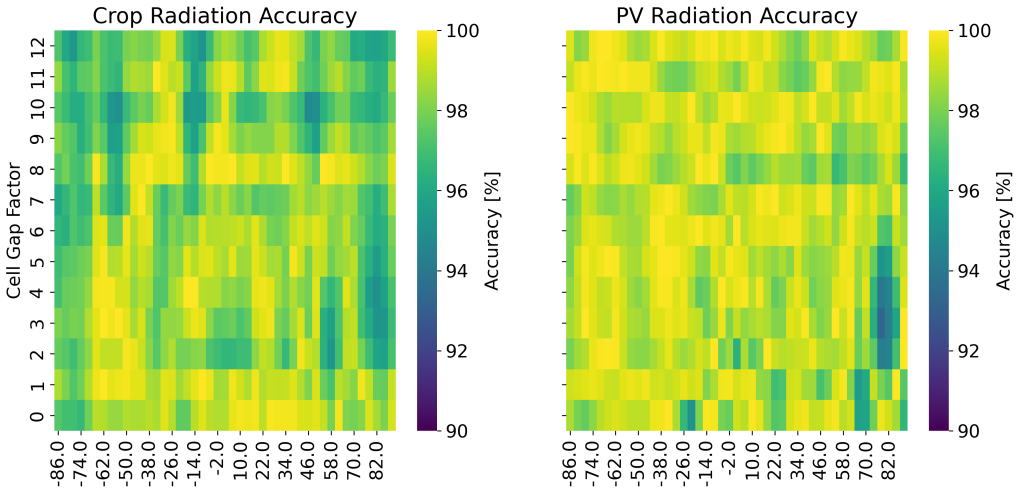

Figure 4.7: Objective functions accuracy, for PAR on Crops and Radiation on Solar Panels compared to classical Radiance values across the design space, for multi objective optimisation.

Figure 4.7 does not display clearly defined regions where accuracy significantly drops for the multi-objective GP model. This is explained by the nature of the acquisition function employed, Expected Hyper-volume Improvement (EHVI), which accounts for two GP models simultaneously. In multi-objective optimisation, the acquisition function aims to expand the Pareto front across the design space, ensuring that no single region is excessively exploited. This leads to a more uniform exploration and prevents the formation of areas with notably poorer performance. The result is a more evenly distributed accuracy profile across the entire design space. This comes at a price that the standard deviations is therefore larger, due to the fact that there is a trade-offs between competing objectives that are characteristic of multi-objective optimisation.

The evolution of mean accuracy for crop and PV radiation per iteration throughout the optimisation process is depicted in Figure 4.8. The graph indicates a steady increase in accuracy during the initial iterations, followed by a plateau as the optimisation progresses. This trend demonstrates the model's rapid convergence to high accuracy, stabilising after gathering sufficient data points. The plateau suggests that additional iterations contribute minimally to further accuracy improvements, indicating an efficient and effective optimisation process. Note that the accuracy for PV radiation stops growing at 99% due to Radiance having a 1% noise.

Figure 4.8 also shows a general lower accuracy for Crop PAR than for PV radiation. This discrepancy might be attributed to the fact that the PV radiation values are twice as large as the PAR values on the crops. Such range differences can induce a bias in the Expected Hyper-volume Improvement (EHVI) acquisition function used in this multi-objective optimisation, as the larger values of PV radiation disproportionately influence the hyper-volume calculation. To mitigate this issue one should normalise the objectives before optimisation.

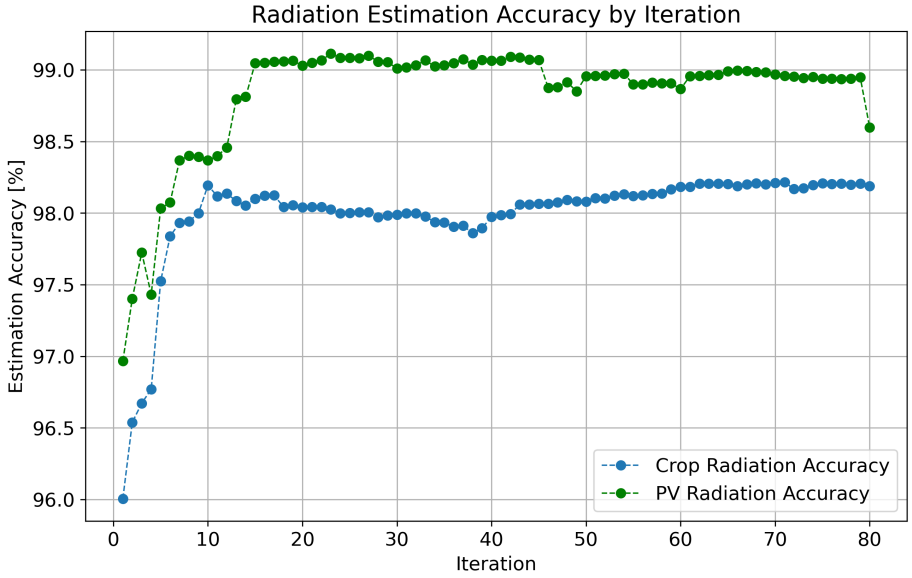

Figure 4.8: Accuracy of the objective functions per iteration in multi-objective optimisation.

4.2.2. Sensitivity Analysis

A sensitivity analysis was conducted to evaluate the impact of input parameters on the performance of the GP models in the multi-objective optimisation algorithm. This involved varying the number of initial samples and exploration levels. The required number of iterations to achieve at least a 95% accuracy, for both objective functions (crop and PV radiation) was recorded, and shown in Table 4.3.

Exploration Level	2 Initial Samples	5 Initial Samples	10 Initial Samples
Low	12	6	<1
Medium	8	5	<1
High	9	5	<1

Table 4.3: Number of iterations necessary to reach a 95% accuracy for both GP models for different levels of exploration and initial samples, for multi-objective optimisation.

The results in Table 4.3 reveal that, increasing the number of initial samples significantly reduces the number of iterations required to reach the desired accuracy, regardless of the exploration level. Furthermore, with 10 initial samples, the required iterations drop to less than one, indicating that the model achieves high accuracy almost immediately. Finally, for 2 initial samples, the iterations needed range from 8 to 12, depending on the exploration level. This suggests that the exploration factor holds a bigger importance with fewer initial samples.

To further analyse the sensitivity, the total number of function evaluations was fixed at 30. This approach allowed for a comparison of the final GP model accuracy across different settings. The accuracy for crop and PV radiation under varying exploration levels and initial samples are presented in Tables 4.4 and 4.5, respectively.

Exploration Level	2 Initial Samples	5 Initial Samples	10 Initial Samples
Low	(97.9 ± 0.9)%	(97.9 ± 1.1)%	(98.0 ± 0.9)%
Medium	(98.1 ± 0.8)%	(97.9 ± 0.8)%	(98.2 ± 0.7)%
High	(97.9 ± 0.8)%	(98.0 ± 0.8)%	(98.0 ± 0.7)%

Table 4.4: GP model accuracy for crop radiation for different levels of exploration and initial samples, for multi-objective optimisation.

Exploration Level	2 Initial Samples	5 Initial Samples	10 Initial Samples
Low	(99.1 ± 0.6)%	(99.0 ± 0.7)%	(99.0 ± 0.7)%
Medium	(99.2 ± 0.5)%	(99.2 ± 0.5)%	(99.2 ± 0.5)%
High	(99.1 ± 0.5)%	(99.2 ± 0.5)%	(99.2 ± 0.6)%

Table 4.5: GP model accuracy for PV radiation for different levels of exploration and initial samples, for multi-objective optimisation.

Tables 4.4 and 4.5 demonstrate that the accuracy slightly improves as the number of initial samples increases across all exploration levels. This trend indicates that a larger initial dataset enhances the surrogate model's ability to predict accurately. The differences in accuracy across different exploration levels are minimal, suggesting that while exploration is necessary to avoid local optima, it does not significantly impact the final accuracy once sufficient data points are collected. Finally, the low standard deviations across all settings indicate consistent model performance, with minor variations in accuracy, affirming the reliability of the GP model no matter the input parameters.

Moreover, with regards to the variation in accuracy across the design space, there is no clear change depending on the input parameters. Similarly, no input parameters seem to impact the difference in accuracy between the crop and PV radiation significantly.

4.2.3. Concluding Remarks

The results demonstrate that, with well-chosen input parameters, the optimisation process can be significantly shortened, achieving 95% accuracy for both objective functions in just one hour. This efficiency, is highlighted in Table 4.3, where only 10 function evaluations are needed for a medium exploration level, regardless of the initial sample count. Even in the most demanding scenarios, the required number of evaluations does not surpass 14. Furthermore, 4.4 and 4.5 illustrate that accuracy of 98.2% for crop PAR and 99.2% for PV radiation can be achieved with just 30 evaluations, showcasing the model's efficiency. These findings demonstrate the effectiveness and robustness of the GP model to varying operational conditions.

5

Optimal Solution(s)

In this chapter, the optimal solutions for both single, Section 5.1 and multi-objective, Section 5.2, optimisation are presented and analysed. A sensitivity analysis is also performed and focuses on how variations in input parameters, such as the number of initial samples and the exploration factor, affect the optimal solution(s).

5.1. Single Objective Optimisation

In this section, the optimal solution obtained using the single-objective optimisation algorithm is presented and analysed, as detailed in Section 5.1.1. Additionally, a sensitivity analysis of this solution is discussed in Section 5.1.2.

5.1.1. Optimal Result

In single-objective optimisation, the optimal solution is a single solution that maximises the objective function, represented by specific values for variables, in this case, tilt and cell gap factor. After conducting 80 iterations with 10 initial samples and a low exploration factor, the optimal solution was found to be at a radiation of $4.32 \cdot 10^5$ kWh for a tilt angle of 6 degrees and a cell gap factor of 1. The evolution of the objective function's value is plotted through the optimisation iterations, in Figure 5.1. One can see that the objective function initially increases, reaching a maximum value at 18 iterations. The algorithm then remains in that region for around 15 iterations, effectively exploiting the area before exploring other potential regions in the design space.

The cumulative maximum of the objective function found through the optimisation loop is plotted in Figure 5.2. It is evident that once the optimal solution found by the 18th iteration, a few comparable solutions were identified in the next 10 iterations, see Figure 5.1 but after that this maximum value was never approached again. This observation indicates that extending the optimisation to 80 iterations might not have been necessary. An alternative, more efficient strategy could involve halting the optimisation sooner, for instance, if no improved solutions are detected after a certain number of iterations. This approach could conserve both time and computational resources. The graph in Figure 5.2, which plots the cumulative optimal points per iteration, further supports this conclusion by showing no improvement beyond the 23rd iteration.

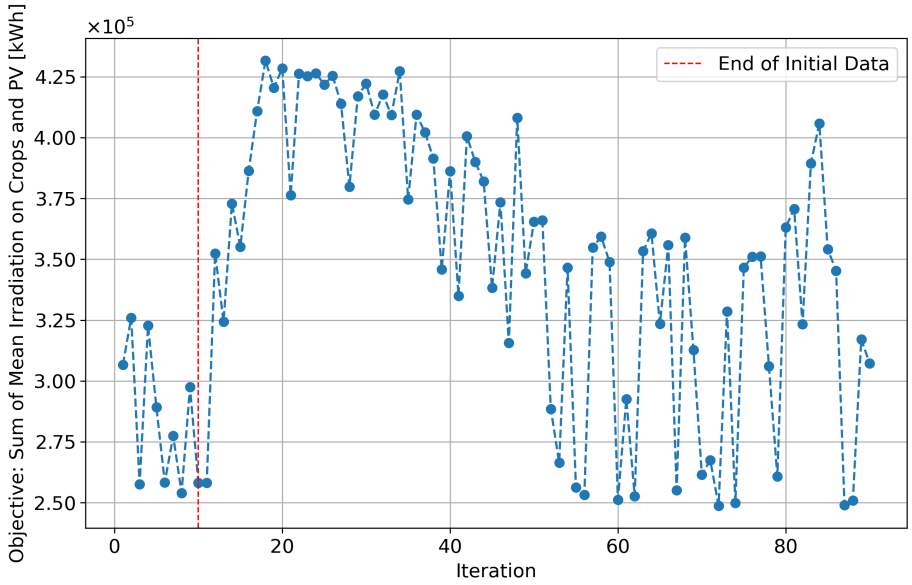

Figure 5.1: Single Objective function, the sum of crop and PV mean radiation, per iteration.

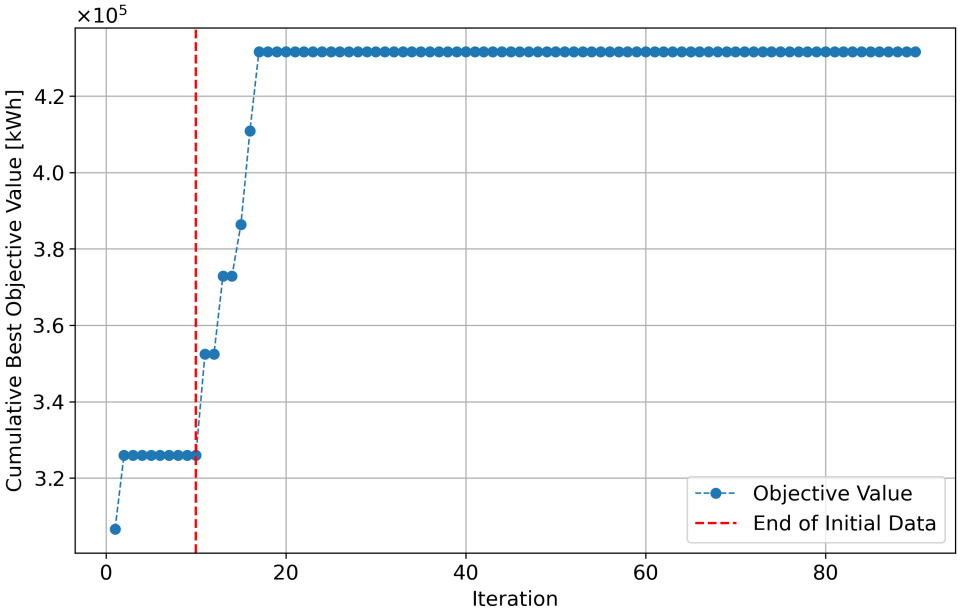

Figure 5.2: Cumulative optimal point per iteration in [kWh], for single objective optimisation.

A representation of the design search space showing the distribution of evaluated points is shown in Figure 5.3. The optimal configuration is situated in the lower central part of the search space, indicating that the highest objective function values consistently emerge from this region, as evidenced in Figure 5.3. This observation is corroborated by the Radiance simulation results shown in Figure 4.1, confirming the location of the optimal region.

This preferred setup, with a nearly horizontal panel tilt of 6 degrees eastward and the narrowest cell gap, maximises sunlight exposure for the PV panels throughout the day while optimising panel area, thus enhancing overall irradiation and power output. However, this arrangement favours PV panel

irradiation significantly over PAR on the crops. The minimal cell gap ensures very little light reaches the crops beneath the panels, evident from the Radiance simulation for crop irradiation (Figure 3.6), which shows minimal crop exposure near a zero tilt angle and a cell gap factor of 1.

This aligns with what was found in Section 2.1.2. Where it was demonstrated that single-objective optimisation focused on combined crop and PV yield can compromise crop health due to inadequate light, with the algorithm prioritising PV output. The disparity could be explained by the fact that the radiation on the PV panels is two times bigger than the radiation received by the crops, a fact discernible only through multi-objective optimisation where crop and PV radiation are evaluated separately.

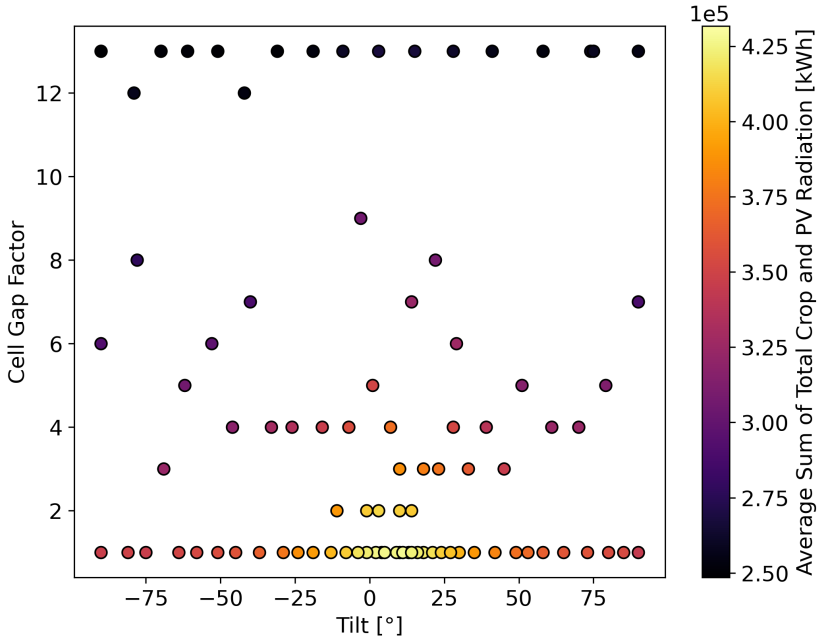

Figure 5.3: Design space with evaluated query points with different tilt and cell gap factors for a low exploration factor, for 80 iterations in single objective optimisation.

To avoid such bias, another optimisation loop was conducted, this time imposing the constraint in Equation 3.3. It was decided that α in this case would be equal to 0.6 which forces the crop radiation to be at least 60% or higher than the radiation value in full sun conditions. In this case, the optimal point was found for a 73-degree tilt angle and a 1 cell gap factor, resulting in an objective function value of $3.59 \cdot 10^5$ kWh, leading to a 17% decrease from the unconstrained optimisation. The query points are shown in Figure 5.4, where one can see which points meet or fail the constraint. The 73 degree angle indeed favours more light penetration into the crop orchard, ensuring sufficient lighting for the crops. However, this requires the user to make an a prior decision by determining the α value before the optimisation, which is crucial for balancing crop and PV performance. This predetermined α value directly influences the optimisation outcomes, highlighting the importance of setting appropriate thresholds.

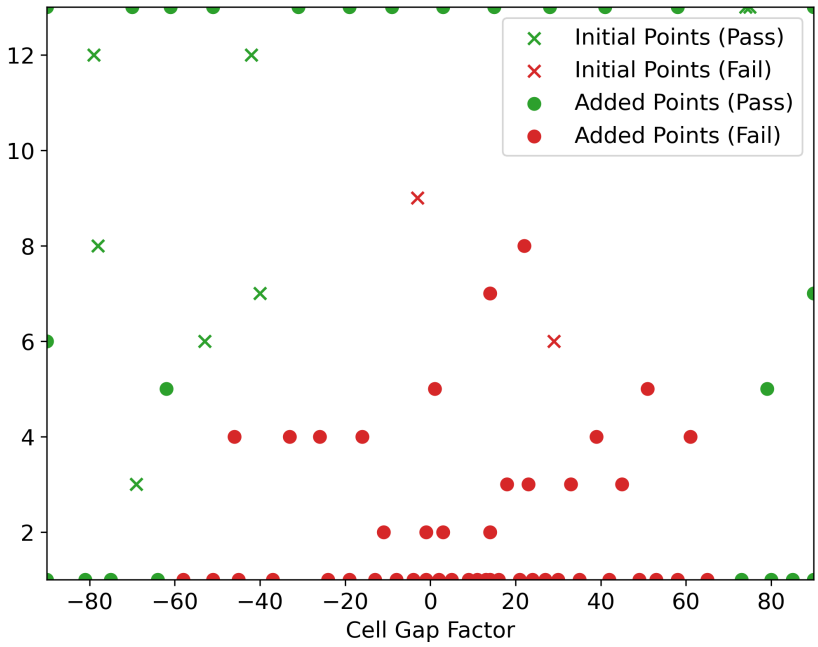

Figure 5.4: Design space with evaluated query points passing or failing crop radiation constraint, for low exploration factor and 80 iterations in single objective optimisation.

5.1.2. Sensitivity Analysis

A sensitivity analysis is conducted to assess the impact of input parameters on the efficiency of the single objective optimisation algorithm in identifying optimal solutions. By keeping the number of objective function evaluations constant while varying the number of initial samples and exploration levels, the corresponding optimal solutions and their parameters were recorded. The results are presented in Table 5.1.

	Exploration Factor	Radiation [kWh]	Tilt [°]	Cell Gap Factor
2 Initial Samples	Low	4.33e5	8	1
	Medium	4.28e5	9	1
	High	4.20e5	-1	1
5 Initial Samples	Low	4.34e5	8	1
	Medium	4.29e5	8	1
	High	4.31e5	3	1
10 Initial Samples	Low	4.33e5	5	1
	Medium	4.27e5	9	1
	High	4.22e5	0	1

Table 5.1: Optimal solutions found by single objective optimisation for different levels of exploration and initial samples in sigle objective optimisation.

The data from Table 5.1 reveals a trend where increasing the number of initial samples generally maintains or slightly improves radiation output, though this is not uniformly the case across all exploration levels. For instance, with low and medium exploration levels, increasing initial samples does not significantly alter radiation values, suggesting that the initial sample size robustly captures the solution space well enough to avoid major deviations in outcome. Regarding the exploration levels, lower exploration levels consistently yield higher radiation outputs across all initial sample sizes, except for the anomaly at 10 initial samples where the medium exploration level results in a decrease in radiation. This suggests that for this specific scenario, less aggressive exploration combined with a higher number of initial samples efficiently converges to near-optimal solutions.

Additionally, the study examined the sensitivity of the optimal single solution using various visual representations. The query points across the search space are shown in Figure 5.5 and 5.6 for a low and high exploration factor,respectively The design space with a low exploration factor (Figure 5.5) displays a more concentrated cluster of query points, suggesting a focused search around perceived optimal regions. Conversely, the high exploration factor (Figure 5.6) results in a more dispersed spread of query points, indicating a broader exploration of the search space. This figure demonstrates that points are tightly clustered around the optimal region with a low exploration factor, enhancing the efficiency of identifying and leveraging optimal solutions. Whereas, in scenarios with medium to high exploration factors, query points are more dispersed across the search space, resulting in fewer evaluations within the most promising areas.

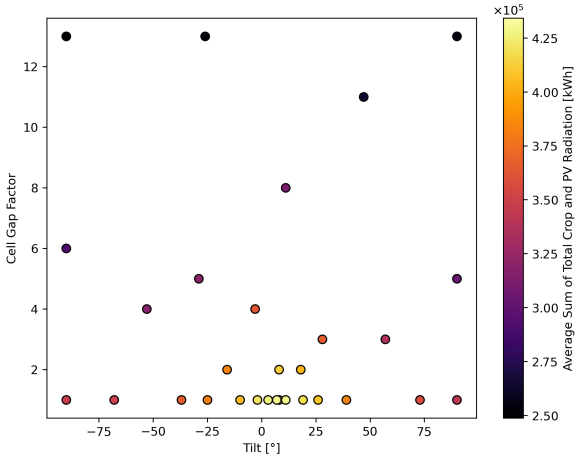

Figure 5.5: Design space including query points for a low exploration factor, in single objective optimisation.

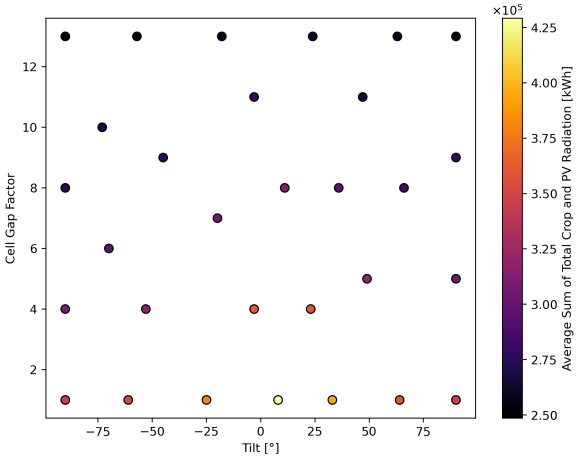

Figure 5.6: Design space including query points for a high exploration factor, in single objective optimisation.

Figure 5.7 depict the objective function values per iteration under low and high exploration factors. A low exploration factor shows a quicker stabilisation of objective values, hinting at faster convergence, whereas the high exploration factor exhibits more fluctuation in objective values, suggesting ongoing exploration and adjustments, leading to a slower convergence. This confirms the previous observation that a low exploration factor is preferable when aiming to find an optimal solution quickly.

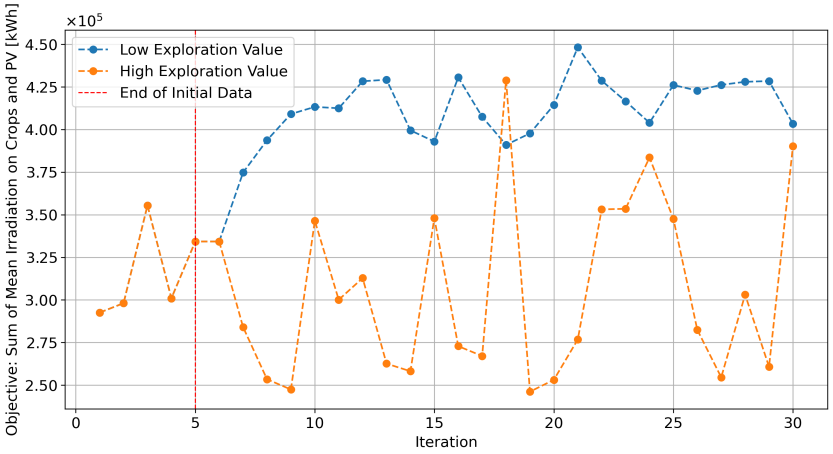

Figure 5.7: Objective function, the sum of crop and PV mean radiation, per iteration for a low and high exploration factor in single objective optimisation.

The cumulative optimal points per iteration for both exploration levels is presented in Figure 5.8. The

lower exploration scenario reaches a maximum after 10 iterations, indicating that optimal points are identified quickly and maintained throughout subsequent iterations. The higher exploration scenario shows a more gradual approach to reaching the same cumulative optimum, as the function continues to rise even after 19 iterations. Which ones again confirms that a lower exploration factor converges faster toward the optimal solution.

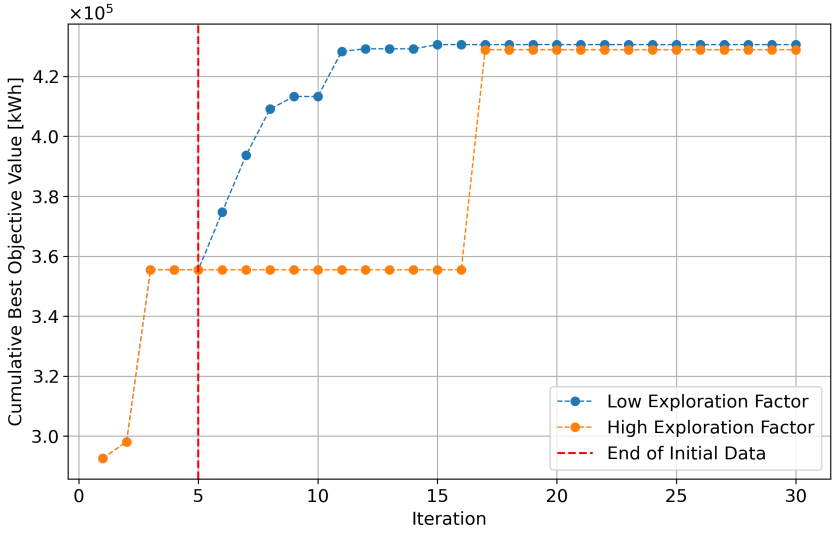

Figure 5.8: Cumulative optimal point per iteration for a low and high exploration factor, in single objective optimisation.

Overall, higher exploration factors allow for extensive exploration of the design space, they may not efficiently exploit the most promising regions as effectively as lower exploration factors. Lower exploration levels enhance the efficiency of identifying and leveraging optimal solutions, indicating a strategic balance is crucial for optimising performance.

5.1.3. Concluding Remarks

The results demonstrate that similar or even superior solutions, achieving higher objective function values, can be reached within just 2.5 hours, compared to the outcomes from an 80 iteration optimisation loop. No matter the input parameters, all optimal solutions fall within a similar order of magnitude, with some surpassing the results from the 80 iteration optimisation loop. Each solution features a cell gap factor of 1, and the tilt angles range between -1 and 9 degrees. Consequently, this suggests that regardless of the input parameters, a solution reasonably close to optimal can be identified within just 30 function evaluations. Though, this optimisation technique appears to favour the radiation on the PV panels over the crop ration, thus to avoid such situation, one should implement a constraint on the maximum crop radiation reduction.

5.2. Multi-Objective Optimisation

In this section, the optimal solutions obtained using the multi-objective optimisation algorithm is presented and analysed, as detailed in Section 5.2.1. Additionally, a sensitivity analysis of these solutions is discussed in Section 5.2.2.

5.2.1. Optimal Results

For multi-objective scenarios, the optimal solutions constitute a set of non-dominated solutions, each representing an optimal layout configuration. These solutions form part of the Pareto front, which can

be visualised by plotting the points in the objective space as shown in Figure 5.9. Figure 5.9 illustrates the Pareto front in the objective space, representing a set of non-dominated solutions for the multi-objective optimisation scenario. The identification of 33 non-dominated points in the 80-iteration optimisation loop demonstrates the algorithm's ability to explore and exploit the design space effectively. Each of these points indicates a configuration of tilt angle and cell gap factor that optimally balances the dual objectives of maximising crop and PV radiation. These solutions are non-dominated, meaning no other solution in the design space can improve one objective without compromising the other. This Pareto front provides a visual representation of the trade-offs between crop and PV radiation, offering stakeholders various options based on their priorities.

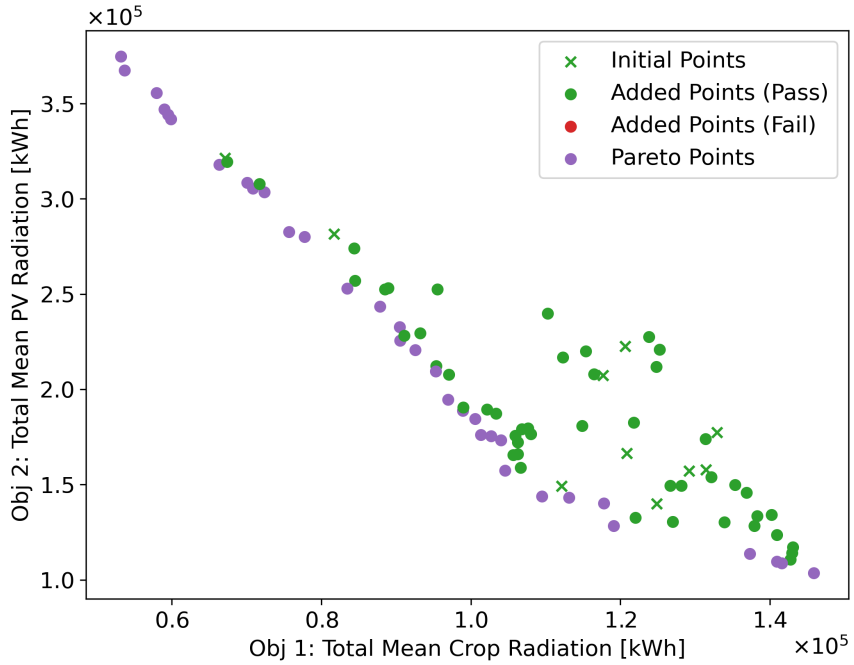

Figure 5.9: Pareto front in the objective space for multi-objective optimisation.

The design space for crop and PV radiation with the non-dominated solutions is depicted in Figure 5.10. These points are scattered throughout the design space, showcasing the diversity of optimal tilt and cell gap combinations. The spread of these points indicates multiple feasible configurations that have achieve Pareto optimum for both objectives. This diversity allows for flexible decision-making, enabling the selection of specific configurations that meet unique requirements or constraints of the agri-PV system.

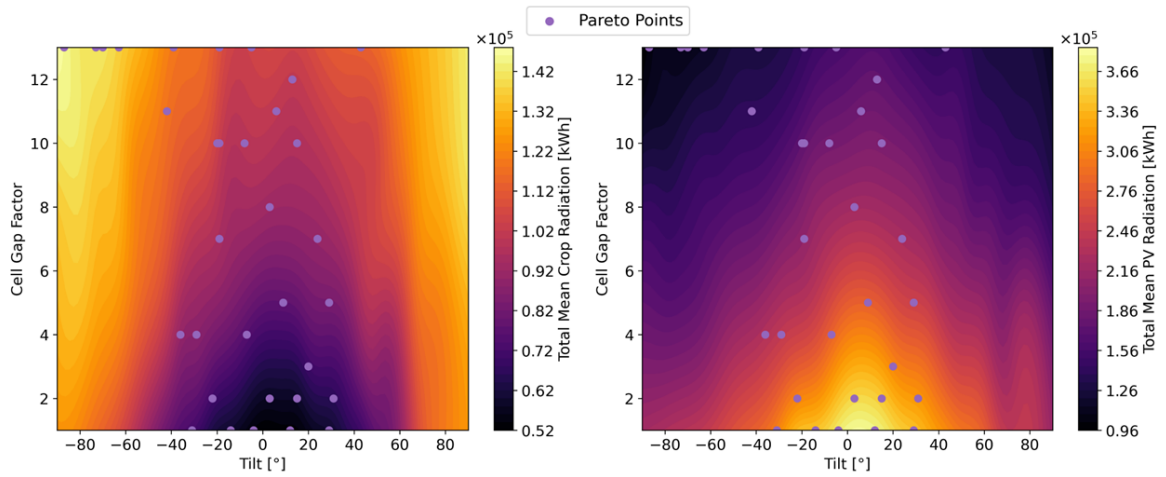

Figure 5.10: Design space for crop and PV radiation with non-dominated solutions (Pareto points).

Finally, the values of each objective function per iteration are plotted in Figure **??**. This figure provides a comprehensive overview of how the objectives evolve over time, demonstrating the convergence behaviour of the optimisation algorithm. It can be observed that crop and PV radiation are inversely correlated, as crop radiation slightly decreases, PV radiation slightly increases. Additionally, both objectives require around 20 to 30 iterations to become more stable, gradually stabilising as the Pareto front is approached.

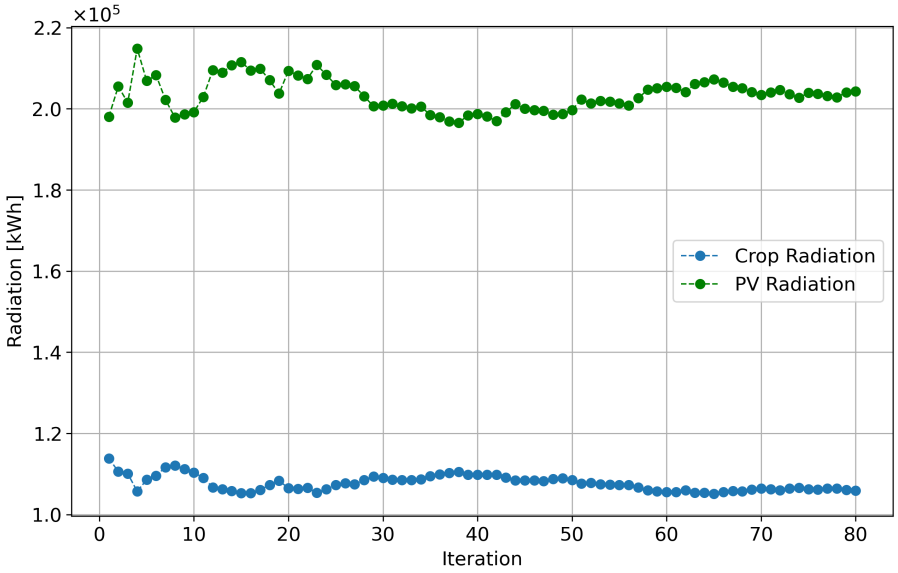

Figure 5.11: Objectives functions per iteration in multi-objective optimisation.

5.2.2. Sensitivity Analysis

A sensitivity analysis is conducted to assess the impact of input parameters on the efficiency of the multi-objective optimisation algorithm in identifying optimal solutions. By keeping the number of objective function evaluations constant to 30,while varying the number of initial samples and exploration levels, the number of non-dominated solution found is recorded. The results are presented in Table 5.2.

Exploration Level	2 Initial Samples	5 Initial Samples	10 Initial Samples
Low	15	15	16
Medium	14	15	14
High	13	13	14

Table 5.2: Number of Non-Dominated solutions found for different levels of exploration and initial samples in multi-objective optimisation.

The results indicate a clear trend: a low exploration factor consistently identifies more non-dominated solutions compared to medium and high exploration levels. This suggests that a lower exploration factor, which focuses more on exploitation, is more effective in finding optimal solutions within a defined design space. Conversely, higher exploration factors, while useful for broadly exploring the design space, may dilute the focus on promising regions, resulting in fewer non-dominated solutions.

Furthermore, increasing the number of initial samples appears to enhance the algorithm's performance marginally. For instance, in the low exploration category, the number of non-dominated solutions increased from 15 with two initial samples to 16 with ten initial samples. This slight improvement suggests that a larger initial dataset helps in better shaping the surrogate model, leading to more effective identification of optimal solutions.

To further analyse the sensitivity of these optimal solutions, the two objectives per iteration were plotted for low and high exploration levels. Figure 5.12 shows the progression of Crop Radiation and PV Radiation per iteration. This figure reveal that with a low exploration factor, the objectives start converging from the 3rd iteration onwards. This initial delay in convergence can be attributed to the need for the model to gather sufficient data points to accurately shape the search space and identify promising regions. Once enough information is collected, the optimisation process rapidly converges to stable values. In contrast, the high exploration factor results in greater variability in objective values per iteration, particularly for PV radiation, reflecting a broader but less focused search that takes longer to converge.

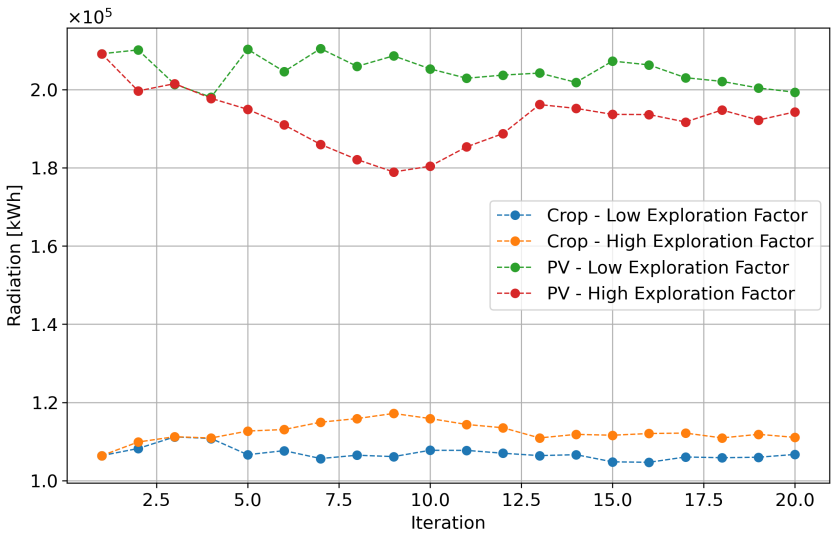

Figure 5.12: Objective Functions per iteration for different levels of exploration factors, in multi-objective optimisation.

No notable differences were noticed regarding the non-dominated solutions spread in the design space depending on the exploration parameter nor the number of initial points. The Pareto front shape also seems consistent across all parameter changes. This consistency can be explained by the fact that the hyper-volume values at the end of all the optimisations with different parameters were always similar. However, what varied was the evolution of the hyper-volume, as seen in Figure 5.13, where the

hyper-volume increases much faster for lower exploration factors than for medium to high exploration factors.

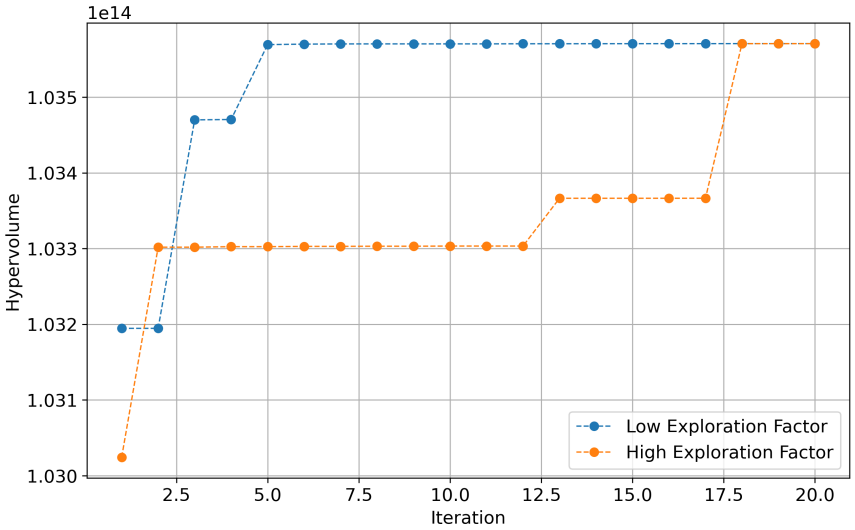

Figure 5.13: Hyper-volume evolution for low and high exploration factors in multi-objective optimisation.

5.2.3. Concluding Remarks

The analysis reveals that input parameters have a limited impact on the number of non-dominated solutions, indicating that the number of iterations plays a more significant role in influencing the outcomes of the optimisation process. Interestingly, the efficiency of the process, measured by the ratio of non-dominated solutions to the total number of objective function evaluations, appears to decrease with an increase in iterations. Specifically, after 30 function evaluations, approximately half of the query points sampled tend to be non-dominated solutions. However, this efficiency diminishes with more extensive evaluations: after 90 function evaluations, only 33 non-dominated solutions are typically identified. This trend suggests that while increasing iterations allows for more thorough exploration of the design space, it does not proportionally enhance the discovery of optimal solutions, highlighting a potential area for optimising the balance between exploration depth and computational efficiency.

6

Comparative Evaluation

In this chapter, a comparative evaluation between single and multi-objective optimisation algorithms is conducted. This evaluation is structured into several key sections: Section 6.1 assesses the convergence speed of both algorithms. Section 6.2 explores the diversity of solutions generated by each algorithm. Section 6.3 examines the robustness of each algorithm, focusing on their performance stability under varying input parameters. Finally, Section 6.4 provides a qualitative evaluation, offering insights into the practical implications and usability of each optimisation approach. This structured analysis aims to delineate the strengths and weaknesses of single versus multi-objective optimisation in various operational contexts.

6.1. Convergence Speed

In single-objective optimisation, the Gaussian Process (GP) model demonstrates rapid convergence, as shown in Figure 4.2, achieving a high accuracy of almost 98.5% after only 3 iterations. This indicates the GP model's ability to quickly adapt and reach high accuracy. However, it should be highlighted that the same figure shows significant accuracy drops at iterations 5 and 71. After the drop at the 5th iteration, the model requires 20 more iterations to recover the previous accuracy level. Regarding the drop at the 70th iteration, the accuracy level is never fully recovered before the end of the optimisation loop.

Conversely, multi-objective optimisation exhibits a more gradual convergence. Despite strong initial convergence, the accuracy stabilises with minimal fluctuations as the process progresses, indicating a comprehensive exploration of the solution space. This method typically requires around 15 iterations, Figure 4.8, to reach a stable accuracy plateau across multiple objectives, reflecting the complexity of balancing competing criteria.

Direct comparison shows that single-objective optimisation converges faster due to its focused nature on optimising a single criterion, often reaching a high accuracy within fewer iterations. Multi-objective optimisation, while initially slower, maintains more stable accuracy levels once they are reached. This stability is beneficial in scenarios where the optimal number of iterations is uncertain, making multi-objective optimisation a more reliable choice when consistent performance is crucial. In contrast, the single-objective approach might experience declines in accuracy when additional query points are evaluated, illustrating the trade-offs between speed and stability in choosing optimisation methods.

6.2. Diversity of Solutions

In single objective optimisation, the diversity of solutions is inherently limited because the goal is to maximise one specific criterion. The results from the GP model in the single objective context reveal a convergence towards a single optimal solution, characterised by a tilt angle of 6 degrees and a cell gap factor of 1. This configuration provides the highest radiation output, effectively fulfilling the singular objective of maximising energy capture. In this case, diversity is not a priority, and the exploration tends

to cluster around the most promising areas, quickly narrowing down to the optimum as evidenced by the design space visualisations.

Multi-objective optimisation, by contrast, inherently supports a higher diversity of solutions due to the need to balance several objectives simultaneously. The results from the GP model in this context showcase a set of non-dominated solutions, forming a Pareto front. Each point on this front represents a different trade-off between the objectives, by maximising crop and PV radiation. The diversity of solutions is evident in the spread of non-dominated points across the design space as shown in Figure 5.10, providing stakeholders with a variety of configurations to choose from based on their specific priorities and constraints.

The fundamental difference in the nature of single and multi-objective optimisations leads to a stark contrast in solution diversity: Single Objective optimisation tends to produce a focused exploration and a narrow set of solutions and multi-Objective optimisation offers a wide array of solutions, each representing different compromises between the objectives, and encourages broader exploration of the design space.

6.3. Robustness

The robustness of the single objective algorithm is tested during sensitivity analysis of the GP model. The model's performance displayed sensitivity to input parameters, as indicated the accuracy fluctuated between 96.0% to 99% depending on the exploration levels and initial sample sizes. Leading to a 3% delta variation depending on the input parameters. Regarding the number of iterations required to achieve at least 95% accuracy, it varied from a total of 27 objective function evaluation to only 7 with different initial conditions, as shown in Table 4.1. This indicates that while the GP model can be highly efficient under optimal conditions, its performance is contingent on the initial setup, which can be viewed as a limitation in terms of robustness.

Multi-objective optimisation, by nature, must balance multiple competing goals, which introduces inherent robustness against over-fitting to a single objective at the expense of others. During the sensitivity analysis of the GP model used for multi-objective optimisation, the accuracy fluctuated from 97.9% to 98.2% for the crop radiation and from 99.0% to 99.2% from the PV radiation. Leading to a 1.3% and 0.2% delta variation depending on the input parameters. Regarding the number of iterations required to achieve at least 95% accuracy, it varied from a total of 14 objective function evaluations to 10 with different initial conditions, as shown in Table 4.3.

The findings suggest that multi-objective optimisation is generally more robust than single objective optimisation in handling variability in initial conditions and maintaining performance across different settings. For decision-makers, this means that employing a multi-objective approach could yield more consistent and reliable outcomes, especially in complex systems where multiple performance criteria are important.

6.4. Qualitative Insights

Interpretability: Multi-objective optimisation provides detailed information about each objective, which is crucial for understanding trade-offs in complex systems. While single-objective optimisation focuses deeply on one criterion, it lacks the broader perspective of multiple objectives. Also, when summing together multiple metrics in single objective function, one can not have information about the individual metrics but only their weighted sum.

Configuration Complexity: Single-objective optimisation is simpler to set up, involving only one objective function and constraints. This makes it more accessible. Multi-objective optimisation is more complex as multiple objectives are defined and it requires more complex tools for the Gaussian model and acquisition function. However, in multi-objective optimisation algorithms, the objectives are easier to define as they do not require to aggregate all the objective together in a weighted sum. Indeed, such decision can be made after the optimisation process.

User Experience: Single-objective optimisation offers a focused user experience, providing clear and single answers, which can be more satisfying and easier to apply. Multi-objective optimisation offers a richer set of solutions but can overwhelm users with choices and complexity without adequate decision-making tools.

Ease of Integration: Integrating single-objective optimisation into broader systems is challenging due to its focus on one objective, making it less flexible for complex systems. It may require predefined weights, introducing bias. Multi-objective optimisation, on the other hand, is more flexible, handling diverse requirements and goals effectively. It allows users to keep performance metrics separate and make decisions based on desired outcomes after the optimisation process.

6.5. Concluding Remarks

Single-objective optimisation demonstrates faster convergence, whereas multi-objective optimisation maintains more consistent accuracy over time. While single-objective optimisation converges toward a single optimal solution, multi-objective optimisation supports a broader range of solutions, accommodating complex decision-making needs. Furthermore, multi-objective optimisation exhibits greater robustness in handling variability in initial conditions and maintaining consistent performance. Although single-objective optimisation is easier to interpret and manage, multi-objective optimisation provides richer insights.

For practical applications, particularly in fields like agri-PV systems where environmental and operational conditions can vary widely, the robustness and comprehensive information output of an optimisation algorithm are crucial. Multi-objective optimisation's ability to adapt and provide balanced solutions across various objectives makes it a preferable choice in such contexts.

7

Critical Analysis and Future Prospects

This chapter provides a critical analysis of the model developed in this study on optimising agri-PV system layouts and outlines future prospects for further advancements. It identifies key limitations of the study, Section 7.1, offers recommendations for future research, Section 7.2, and discusses the practical implications and potential benefits from a farmer's perspective, Section 7.3.

7.1. Limitations

This study provides valuable insights into optimising agri-PV system layouts but has notable limitations, the main one are elaborated in this section.

Firstly, a significant limitation is the model's exclusive focus on radiation values without accounting for crop yield and electricity production. This focus introduces a discrepancy, as the optimisation outcomes differ from those that would emerge if crop and electricity yields were included in the optimisation. Indeed, the conversion efficiency of converting radiation to electricity through PV panels is higher than the efficiency of converting Photosynthetically Active Radiation (PAR) to crop yield, introducing further bias in the optimisation and impacting the optimal solutions found, which might no longer be optimal.

Focusing solely on optimising the agri-PV layout based on radiance introduced another limitation. Indeed, the irradiation values were converted to radiation by multiplying them by the active surface area of the PV modules and the crops. For PV modules, this calculation was straightforward, involving the surface area of each solar cell. However, estimating this for crops was complex, as it required considering the active and collective surface area of trees, which is comprised of multiple leaves with different sizes, orientations, colours, and densities (Tokarz et al., 2013). Consequently, the active area of the trees was an approximation.

Thirdly, he simulations use annual mean values, which overlooks the diurnal and seasonal variations in solar exposure. This limitation hinders a comprehensive understanding of the Photosynthetically Active Radiation (PAR) available to plants and fails to illustrate how PAR incident on crop fluctuates throughout different times of the day or seasons. These variations are critical for optimising light availability for both crop growth and solar power generation.

Regarding the optimisation algorithm, some limitations are linked to the fact that the thesis applied the algorithm to only one case study. Therefore, the behavioural changes of the Bayesian optimisation algorithm were not assessed if additional design variables or objective functions were included. A clear limitation is that with only two variables, it is easy to represent the design space and the objective functions in a colour map, and with three variables, it is still possible to represent them in a 3D plot. However, beyond that point, it is not feasible, making it difficult to assess the general trends when the variables change. Furthermore, if the objective functions are more complicated, for example, with multiple local maxima, the efficiency of the algorithm could be drastically reduced.

Finally, the current research framework does not include essential environmental variables such as

water availability, temperature fluctuations, and wind speed. These factors are crucial for a thorough understanding of the dynamics of agri-PV systems as they significantly influence both crop yield and PV performance. Recognising these limitations is vital for guiding future research that could address these gaps, leading to more refined and accurate optimisation of agri-PV systems.

7.2. Recommendations and Future Work

The following improvements are proposed to extend the current research and address emerging challenges:

The complexity of agri-PV systems suggests a multitude of influencing factors. Future research could benefit from incorporating a broader set of variables that impact the layout and efficiency of these systems such as various glass cover materials used for the PV modules. Additionally, water management is a critical component of sustainable agricultural practices. Incorporating objective functions related to water usage could help in designing systems that not only optimise energy production but also conserve water resources.

Current models often simulate on an annual basis, which may overlook short-term dynamics and interactions between solar energy generation and crop growth. By simulating these processes at an hourly rate, the model could more accurately reflect the dynamic variations in energy production and agricultural needs. To further refine the optimisation model, dedicated sub-models for PV electricity output and crop yield should be developed. These models would enable a more accurate prediction of the energy production capabilities of the PV modules and the potential agricultural yield under different configurations. This approach would allow for a more tailored PV system design that is based on a more thorough performed assessment.

Future iterations of the model could include constraints that focus on maximising electricity production during peak demand times or optimising yield throughout the year. This could be particularly beneficial in regions with seasonal variations in energy demand or agricultural output. By addressing these areas, future research can significantly enhance the efficacy and sustainability of agri-PV systems, leading to more optimised solutions that balance energy production with agricultural productivity.

Future work regarding the optimisation algorithm, should focus on applying the model to multiple case studies to better understand its behavioural changes when additional design variables or objective functions are included. Expanding the scope of the algorithm to handle more than three variables is crucial, as it will enable a more comprehensive representation and analysis of the design space. Advanced visualisation techniques or dimensional reduction methods could be explored to facilitate the assessment of general trends in higher-dimensional spaces. Additionally, developing strategies to improve the algorithm's efficiency in handling complex objective functions with multiple local maxima will be essential. This could involve enhancing the Bayesian optimisation process or integrating hybrid approaches that combine different optimisation techniques.

7.3. Farmer's Perspective and Considerations

The multi-objective optimisation algorithm and its model can be used for two main purposes. First, the model provides users with insights into the general tendencies of various variables within the agri-PV system. This broader understanding allows farmers to see how changes can impact overall system performance. Notably, within one hour, the model can achieve 95% accuracy, a substantial improvement over the four days required to obtain similar results using classical Radiance simulations. This capability enables multi-site (location) analysis within a single day, as well as multi-layout analysis, making it highly convenient in the early stages of the design phase. Users can quickly discern trends and make informed general decisions. This feature provides valuable insights into the performance of agri-PV systems throughout the year, enabling farmers to optimise their systems efficiently and effectively.

Secondly, by employing a low exploration factor, the algorithm can generate up to 15 non-dominated solutions within two hours. These solutions represent potential optimal agri-PV layouts. Since multiple solutions are provided, farmers can make posterior decisions about which solution to pick. For instance,

they can decide the proportion of crop radiation to maintain, possibly choosing a lower tilt angle for more crop shelter or a higher angle for better precipitation management. Farmers can also consider limitation from PV module suppliers on possible cell gap factors.

The model is easily adaptable, allowing farmers to incorporate additional variables and customise objective functions according to their specific requirements. This flexibility is crucial for obtaining a comprehensive overview of a problem with many variables, providing a precise idea of where the optimal layout might be. This approach eliminates the need for real-life measurements and experiments, offering high precision in a very short time.

However, for effective use of this model, certain conditions must be met. At a minimum, users will require training to understand and utilise the optimisation algorithm properly. Additionally, developing a user-friendly or user-oriented interface could significantly enhance accessibility, making it easier for farmers to input their specific parameters and interpret the results without needing extensive technical knowledge. This would ensure that the model's benefits can be fully realised in practical, real-world applications.

8

Conclusion

This thesis examined the optimisation of agri-PV system layouts using a multi-objective approach, focusing on maximising both crop Photosynthetically Active Radiation (PAR) and PV radiation. The primary objective was to optimise the system by maintaining separate goals for crops and PV modules, thereby avoiding inter-connectivity between these conflicting metrics during the optimisation process. To assess the impact of this separation, a single-objective optimisation was conducted in parallel by combining the two conflicting objectives. Additionally, this thesis integrated Radiance, to accurately simulate complex agri-PV system layouts. However, the use of such software presented challenges, as the simulations were computationally intensive and exhibited stochastic behaviour.

The thesis explored three main areas. It identified an effective optimisation algorithm for integration with Radiance. Assess the advantages of using optimisation methodologies over classical Radiance-based ray-tracing simulations. Finally, the effectiveness of multi-objective and single-objective optimisation approaches were compared.

The literature review revealed that Bayesian multi-objective optimisation using a Gaussian Process model was the most suitable choice as it is capable of building a surrogate model with a small number of Radiance evaluations, handling black-box and stochastic behaviour, and most importantly, it is highly efficient, minimising the number of simulations required to optimise the given agri-PV layout.

Regarding the advantages of optimisation methodologies over classical Radiance-based ray-tracing, the results demonstrated that the objective function(s) could be approximated with 95% accuracy within one hour, requiring as few as six objective function evaluations with appropriate input parameters, such as a medium to high exploration factor. This efficiency represents a significant improvement over traditional methods, which require substantially more time (over 4 days) and evaluations (around 600). Furthermore, it was shown that not only is the GP model highly accurate, but the same optimisation loop also provides accurate optimal solutions simultaneously. These optimal solutions represent clear and effective agri-PV layouts.

Finally, the analysis revealed that while single-objective optimisation demonstrates faster convergence, multi-objective optimisation maintains more consistent accuracy and supports a broader range of solutions, accommodating complex decision-making needs. Furthermore, multi-objective optimisation exhibited greater robustness in handling variability in initial conditions and maintaining consistent performance.

Future research should incorporate sub-models for PV electricity output and crop yield, and adopting an hourly simulation basis could provide more detailed and actionable insights. Additionally, the annual simulation approach overlooks diurnal and seasonal variations, and essential environmental variables such as water availability and temperature fluctuations were not included. Recognising these limitations is crucial for guiding future research that could address these gaps.

Overall, this model aids in accelerating the design and optimisation of agri-PV systems, providing a simple, rapid, and accurate tool that elucidates the complexities of these systems. It facilitates the

implementation of agri-PV across orchard fields, demonstrating its potential to optimise both crop and PV performance. This work promotes sustainable development in both the agriculture and renewable energy sectors and contributes by employing a novel multi-objective approach using a highly accurate light model. For end users like farmers, it provides a tool to quickly identify and compare different agri-PV system layouts at various locations.

References

Ahmed, H., & Glasgow, J. (2012). Swarm Intelligence: Concepts, Models and Applications.

Alizadeh, M., Fernandez-Marques, J., Lane, N. D., & Gal, Y. (2019). AN EMPIRICAL STUDY OF BINARY NEURAL NETWORKS' OPTIMISATION.

Amaducci, S., Yin, X., & Colauzzi, M. (2018). Agrivoltaic systems to optimise land use for electric energy production. *Applied Energy*, *220*, 545–561. https://doi.org/https://doi.org/10.1016/j.apenergy.2018.03.081

Attaviriyanupap, P., Tokuhara, K., Itaya, N., Marmiroli, M., Tsukamoto, Y., & Kojima, Y. (2011). Estimation of photovoltaic power generation output based on solar irradiation and frequency classification. *2011 IEEE PES Innovative Smart Grid Technologies*, 1–7. https://doi.org/10.1109/ISGT-Asia.2011.6167078

Audet, C., Savard, G., & Zghal, W. (2008). Multiobjective Optimization Through a Series of Single-Objective Formulations. https://doi.org/10.1137/060677513

Bechikh, S., Datta, R., & Gupta, A. (Eds.). (2017). *Recent Advances in Evolutionary Multi-objective Optimization* (Vol. 20). Springer International Publishing. https://doi.org/10.1007/978-3-319-42978-6

Beck, M., Bopp, G., Goetzberger, A., Obergfell, T., Reise, C., & Schindele, S. (2012, January). *Combining PV and Food Crops to Agrophotovoltaic ? Optimization of Orientation and Harvest*. https://doi.org/10.4229/27thEUPVSEC2012-5AV.2.25

Beume, N., Naujoks, B., & Emmerich, M. (2006). SMS-EMOA: Multiobjective selection based on dominated hypervolume. *European Journal of Operational Research*. https://doi.org/10.1016/j.ejor.2006.08.008

Boyle, P. (2007, January). *Gaussian Processes for Regression and Optimisation* [thesis]. Open Access Te Herenga Waka-Victoria University of Wellington. https://doi.org/10.26686/wgtn.16934869.v1

Buhmann, M. D. (2000). Radial basis functions. *Acta Numerica*, *9*, 1–38. https://doi.org/10.1017/S0962492900000015

Campana, P. E., Stridh, B., Amaducci, S., & Colauzzi, M. (2021). Optimisation of vertically mounted agrivoltaic systems. *Journal of Cleaner Production*, *325*, 129091. https://doi.org/https://doi.org/10.1016/j.jclepro.2021.129091

Carreño-Ortega, A., do Paço, T. A., Díaz-Pérez, M., & Gómez-Galán, M. (2021). Lettuce Production under Mini-PV Modules Arranged in Patterned Designs [Number: 12 Publisher: Multidisciplinary Digital Publishing Institute]. *Agronomy*, *11*(12), 2554. https://doi.org/10.3390/agronomy11122554

Chahar, V., & Sharma, S. (2022). A Comprehensive Review on Multi-Objective Optimization Techniques: Past, Present, and Future. *Archives of Computational Methods in Engineering*.

Chand, S., & Wagner, M. (2015). Evolutionary many-objective optimization: A quick-start guide. *Surveys in Operations Research and Management Science*, *20*, 35–42. https://doi.org/10.1016/j.sorms.2015.08.001

Cho, J.-H., Wang, Y., Chen, I.-R., Chan, K. S., & Swami, A. (2017). A Survey on Modeling and Optimizing Multi-Objective Systems. *IEEE Communications Surveys & Tutorials*, *19*(3), 1867–1901. https://doi.org/10.1109/COMST.2017.2698366

Coello, C. A. C. (2011). An Introduction to Multi-Objective Particle Swarm Optimizers. In A. Gaspar-Cunha, R. Takahashi, G. Schaefer, & L. Costa (Eds.), *Soft Computing in Industrial Applications* (pp. 3–12). Springer. https://doi.org/10.1007/978-3-642-20505-7_1

Deb, K., Pratap, A., Agarwal, S., & Meyarivan, T. (2002). A fast and elitist multiobjective genetic algorithm: NSGA-II. *IEEE Transactions on Evolutionary Computation*, *6*(2), 182–197. https://doi.org/10.1109/4235.996017

Dupraz, C., Marrou, H., Talbot, G., Dufour, L., Nogier, A., & Ferard, Y. (2011). Combining solar photovoltaic panels and food crops for optimising land use: Towards new agrivoltaic schemes. *Renewable Energy*, *36*(10), 2725–2732. https://doi.org/10.1016/j.renene.2011.03.005

Edgeworth, F. Y. (1881). *Mathematical Psychics: An Essay on the Application of Mathematics to the Moral Sciences* [Google-Books-ID: s7cJAAAAIAAJ]. C. K. Paul.

Elborg, M. (2017, April). *Reducing Land Competition for Agriculture and Photovoltaic Energy Generation-A Comparison of Two Agro-Photovoltaic Plants in Japan*. https://doi.org/10.21275/1081704

Emmerich, M. T. M., & Deutz, A. H. (2018). A tutorial on multiobjective optimization: Fundamentals and evolutionary methods. *Natural Computing*, *17*(3), 585–609. https://doi.org/10.1007/s11047-018-9685-y

Emmerich, M., Giannakoglou, K., & Naujoks, B. (2006). Single- and multiobjective evolutionary optimization assiste. Retrieved June 21, 2024, from https://ieeexplore.ieee.org/document/1665031

European Commission. Joint Research Centre. (2023). *Overview of the potential and challenges for agri-photovoltaics in the European Union.* Publications Office. Retrieved June 11, 2024, from https://data.europa.eu/doi/10.2760/208702

Falcón-Cardona, J. G., & Coello, C. A. C. (2019). Convergence and diversity analysis of indicator-based multi-objective evolutionary algorithms. *Proceedings of the Genetic and Evolutionary Computation Conference*, 524–531. https://doi.org/10.1145/3321707.3321718

Forrester, A., Sóbester, A., & Keane, A. (2008, September). *Engineering Design via Surrogate Modelling: A Practical Guide* [Google-Books-ID: ulMHmeMnRCcC]. John Wiley & Sons.

Frazier, P. I. (2018, July). A Tutorial on Bayesian Optimization [arXiv:1807.02811 [cs, math, stat]]. Retrieved May 22, 2024, from http://arxiv.org/abs/1807.02811

Frean, M., & Boyle, P. (2008). Using Gaussian Processes to Optimize Expensive Functions. In W. Wobcke & M. Zhang (Eds.), *AI 2008: Advances in Artificial Intelligence* (pp. 258–267). Springer. https://doi.org/10.1007/978-3-540-89378-3_25

Goetzberger, A., & Zastrow, A. (1981). On the Coexistence of Solar-Energy Conversion and Plant Cultivation. https://doi.org/10.1080/01425918208909875

Gorjian, S., Bousi, E., Özdemir, Ö. E., Trommsdorff, M., Kumar, N. M., Anand, A., Kant, K., & Chopra, S. S. (2022). Progress and challenges of crop production and electricity generation in agrivoltaic systems using semi-transparent photovoltaic technology. *Renewable and Sustainable Energy Reviews*, *158*, 112126. https://doi.org/https://doi.org/10.1016/j.rser.2022.112126

Gramacy, R. B. (2020). Surrogates | Gaussian Process Modeling, Design, and Optimization for t. Retrieved June 18, 2024, from https://www.taylorfrancis.com/books/mono/10.1201/9780367815493/surrogates-robert-gramacy

Gutmann, H.-M. (2001). A Radial Basis Function Method for Global Optimization. *Journal of Global Optimization*, *19*(3), 201–227. https://doi.org/10.1023/A:1011255519438

Hupkens, I., Emmerich, M., & Deutz, A. (2014, August). Faster Computation of Expected Hypervolume Improvement [arXiv:1408.7114 [cs]]. https://doi.org/10.48550/arXiv.1408.7114

Jiang, P., Zhou, Q., & Shao, X. (2019). Surrogate-Model-Based Design and Optimization | SpringerLink. Retrieved June 18, 2024, from https://link.springer.com/chapter/10.1007/978-981-15-0731-1_7

Jones, D. R., Schonlau, M., & Welch, W. J. (1998). Efficient Global Optimization of Expensive Black-Box Functions. *Journal of Global Optimization*, *13*(4), 455–492. https://doi.org/10.1023/A:1008306431147

Kitayama, S., Srirat, J., Arakawa, M., & Yamazaki, K. (2013). Sequential approximate multi-objective optimization using radial basis function network. *Structural and Multidisciplinary Optimization*, *48*(3), 501–515. https://doi.org/10.1007/s00158-013-0911-z

Knowles, J. (2006). ParEGO: A hybrid algorithm with on-line landscape approximation for expensive multiobjective optimization problems. *IEEE Transactions on Evolutionary Computation*, *10*(1), 50–66. https://doi.org/10.1109/TEVC.2005.851274

Kuhn, H. W., & Tucker, A. (1951). *Proceedings of the Second Berkeley Symposium on Mathematical Statistics and Probability* (J. Neyman).

Kuo, C.-F. J., Su, T.-L., Huang, C.-Y., Liu, H.-C., Barman, J., & Kar, I. (2023). Design and Development of a Symbiotic Agrivoltaic System for the Coexistence of Sustainable Solar Electricity Generation and Agriculture [Number: 7 Publisher: Multidisciplinary Digital Publishing Institute]. *Sustainability*, *15*(7), 6011. https://doi.org/10.3390/su15076011

Kushner, H. J. (1964). A New Method of Locating the Maximum Point of an Arbitrary Multipeak Curve in the Presence of Noise. *Journal of Basic Engineering*, *86*(1), 97–106. https://doi.org/10.1115/1.3653121

Kwon, O.-H., & Lee, K.-S. (2021). Agrophotovoltaic Designs : Irradiation Analysis on and under PV Modules. *Journal of the Korean Solar Energy Society*, *41*(2), 9–23. https://doi.org/10.7836/kses.2021.41.2.009

Laue, T. (2022). *Using ray tracing to model agri-PV greenhouse energy production and PAR levels* [Master's thesis] [Accepted: 2022-09-16T22:00:04Z]. Retrieved June 18, 2024, from https://www.duo.uio.no/handle/10852/96695

Laumanns, M., & Ocenasek, J. (2002). Bayesian Optimization Algorithms for Multi-objective Optimization. In J. J. M. Guervós, P. Adamidis, H.-G. Beyer, H.-P. Schwefel, & J.-L. Fernández-Villacañas (Eds.), *Parallel Problem Solving from Nature — PPSN VII* (pp. 298–307). Springer. https://doi.org/10.1007/3-540-45712-7_29

Lavinas, Y., Ladeira, M., & Aranha, C. (2021, December). Faster Convergence in Multi-Objective Optimization Algorithms Based on Decomposition [arXiv:2112.11939 [cs]]. Retrieved May 1, 2024, from http://arxiv.org/abs/2112.11939

Madsen, J. I., Shyy, W., & Haftka, R. T. (2000). Response Surface Techniques for Diffuser Shape Optimization [Publisher: American Institute of Aeronautics and Astronautics _eprint: https://doi.org/10.2514/2.1160]. *AIAA Journal*, *38*(9), 1512–1518. https://doi.org/10.2514/2.1160

Marglin, S. A. (1967). *Public Investment Criteria (Routledge Revivals): Benefit-Cost Analysis for Planned Economic Growth*. Routledge. https://doi.org/10.4324/9781315737126

Marler, R., & Arora, J. (2004). Survey of Multi-Objective Optimization Methods for Engineering. *Structural and Multidisciplinary Optimization*, *26*, 369–395. https://doi.org/10.1007/s00158-003-0368-6

Marrou, H., Dufour, L., & Wery, J. (2013). How does a shelter of solar panels influence water flows in a soil–crop system? *European Journal of Agronomy*, *50*, 38–51. https://doi.org/https://doi.org/10.1016/j.eja.2013.05.004

Martín-Chivelet, N. (2016). Photovoltaic potential and land-use estimation methodology. *Energy*, *94*, 233–242. https://doi.org/10.1016/j.energy.2015.10.108

McCree, K. J. (1981). Photosynthetically Active Radiation. In O. L. Lange, P. S. Nobel, C. B. Osmond, & H. Ziegler (Eds.), *Physiological Plant Ecology I: Responses to the Physical Environment* (pp. 41–55). Springer. https://doi.org/10.1007/978-3-642-68090-8_3

Mead, R., & Willey, R. W. (1980). The Concept of a 'Land Equivalent Ratio' and Advantages in Yields from Intercropping. *Experimental Agriculture*, *16*(3), 217–228. https://doi.org/10.1017/S0014479700010978

Melkumyan, A., & Ramos, F. (2006). Multi-Kernel Gaussian Processes.

Mengi, E., Samara, O. A., & Zohdi, T. I. (2023). Crop-driven optimization of agrivoltaics using a digital-replica framework. *Smart Agricultural Technology*, *4*, 100168. https://doi.org/https://doi.org/10.1016/j.atech.2022.100168

Mockus, J. (1974). On Bayesian Methods for Seeking the Extremum. *Proceedings of the IFIP Technical Conference*, 400–404.

Oleskewicz, K. (2020). The Effect of Gap Spacing Between Solar Panel Clusters on Crop Biomass Yields, Nutrients, and the Microenvironment in a Dual-Use Agrivoltaic System. *Masters Theses*. https://doi.org/https://doi.org/10.7275/15996616

Peter Frazier, I. (2018). Bayesian Optimization. *INFORMS Tutorials in Operations Research*. https://doi.org/10.1287/educ.2018.0188

Picheny, V. (2015). Multiobjective optimization using Gaussian process emulators via stepwise uncertainty reduction. *Statistics and Computing*, *25*(6), 1265–1280. https://doi.org/10.1007/s11222-014-9477-x

Queipo, N. V., Haftka, R. T., Shyy, W., Goel, T., Vaidyanathan, R., & Kevin Tucker, P. (2005). Surrogate-based analysis and optimization. *Progress in Aerospace Sciences*, *41*(1), 1–28. https://doi.org/10.1016/j.paerosci.2005.02.001

Rajani, Kumar, D., & Kumar, V. (2020). Impact of Controlling Parameters on the Performance of MOPSO Algorithm. *Procedia Computer Science*, *167*, 2132–2139. https://doi.org/10.1016/j.procs.2020.03.261

Rasmussen, C. E., & Williams, C. K. I. (2008). *Gaussian processes for machine learning* (3. print). MIT Press.

Reasoner, M., & Ghosh, A. (2022). Agrivoltaic Engineering and Layout Optimization Approaches in the Transition to Renewable Energy Technologies: A Review [Number: 2 Publisher: Multidisciplinary Digital Publishing Institute]. *Challenges*, *13*(2), 43. https://doi.org/10.3390/challe13020043

Robinson, D., & Stone, A. (2004). Irradiation modelling made simple: The cumulative sky approach and its applications.

Sargentis, G.-F., Siamparina, P., Sakki, G.-K., Efstratiadis, A., Chiotinis, M., & Koutsoyiannis, D. (2021). Agricultural Land or Photovoltaic Parks? The Water–Energy–Food Nexus and Land Development Perspectives in the Thessaly Plain, Greece [Number: 16 Publisher: Multidisciplinary Digital Publishing Institute]. *Sustainability*, *13*(16), 8935. https://doi.org/10.3390/su13168935

Schutze, O., Esquivel, X., Lara, A., & Coello, C. A. C. (2012). Using the Averaged Hausdorff Distance as a Performance Measure in Evolutionary Multiobjective Optimization. *IEEE Transactions on Evolutionary Computation*, *16*(4), 504–522. https://doi.org/10.1109/TEVC.2011.2161872

Schwefel, H. (1965). Kybernetische Evolution als Stratgie der Experimentellen Forschung in der Stromungstechnk. *Diploma Thesis, Tech. Univ. of Berlin*. Retrieved June 18, 2024, from https://cir.nii.ac.jp/crid/1572824499516724480

Shahriari, B., Swersky, K., Wang, Z., Adams, R. P., & De Freitas, N. (2016). Taking the Human Out of the Loop: A Review of Bayesian Optimization. *Proceedings of the IEEE*, *104*(1), 148–175. https://doi.org/10.1109/JPROC.2015.2494218

Snoek, J., Larochelle, H., & Adams, R. P. (2012). Practical Bayesian Optimization of Machine Learning Algorithms. *Advances in Neural Information Processing Systems*, *25*. Retrieved June 21, 2024, from https://proceedings.neurips.cc/paper_files/paper/2012/hash/05311655a15b75fab86956663e1819cd-Abstract.html

Sumin, K., & Sojung, K. (2023). Optimization of the design of an agrophotovoltaic system in future climate conditions in South Korea. *Renewable Energy*, *206*, 928–938. https://doi.org/10.1016/j.renene.2023.02.090

Tabatabaei, M., Hakanen, J., Hartikainen, M., Miettinen, K., & Sindhya, K. (2015). A survey on handling computationally expensive multiobjective optimization problems using surrogates: Non-nature inspired methods. *Structural and Multidisciplinary Optimization*, *52*(1), 1–25. https://doi.org/10.1007/s00158-015-1226-z

Tahir, Z., & Zafar Butt, N. (2021, September). Spatial-Temporal Shading Under Mobile & Fixed Tilt Bifacial Agrivoltaic Panels & Implications for the Cropping Practices. https://doi.org/10.2139/ssrn.3918961

Tang, J., Liu, G., & Pan, Q. (2021). A Review on Representative Swarm Intelligence Algorithms for Solving Optimization Problems: Applications and Trends [Conference Name: IEEE/CAA Journal of Automatica Sinica]. *IEEE/CAA Journal of Automatica Sinica*, *8*(10), 1627–1643. https://doi.org/10.1109/JAS.2021.1004129

Tipu, A. J. S., Conbhuí, P. Ó., & Howley, E. (2024). Artificial neural networks based predictions towards the auto-tuning and optimization of parallel IO bandwidth in HPC system. *Cluster Computing*, *27*(1), 71–90. https://doi.org/10.1007/s10586-022-03814-w

Tokarz, K., Pilarski, J., & Kocurek, M. (2013). The Photosynthetic Surface Area of Apple Trees. In T. Kuang, C. Lu, & L. Zhang (Eds.), *Photosynthesis Research for Food, Fuel and the Future* (pp. 818–824). Springer. https://doi.org/10.1007/978-3-642-32034-7_174

Toledo, C., & Scognamiglio, A. (2021). Agrivoltaic Systems Design and Assessment: A Critical Review, and a Descriptive Model towards a Sustainable Landscape Vision (Three-Dimensional Agrivoltaic Patterns) [Number: 12 Publisher: Multidisciplinary Digital Publishing Institute]. *Sustainability*, *13*(12), 6871. https://doi.org/10.3390/su13126871

Toyoda, T., Yajima, D., Araki, K., & Nishioka, K. (2023). Design Optimization of Agri-Photovoltaic Systems in Different Climate Regions† [_eprint: https://onlinelibrary.wiley.com/doi/pdf/10.1002/tee.23943]. *IEEJ Transactions on Electrical and Electronic Engineering*, *n/a*(n/a). https://doi.org/10.1002/tee.23943

Trommsdorff, M. (2019, April). Agrophotovoltaics: High Harvesting Yield in Hot Summer of 2018 - Fraunhofer ISE. Retrieved March 5, 2024, from https://www.ise.fraunhofer.de/en/press-media/press-releases/2019/agrophotovoltaics-hight-harvesting-yield-in-hot-summer-of-2018.html

Trommsdorff, M., Kang, J., Reise, C., Schindele, S., Bopp, G., Ehmann, A., Weselek, A., Högy, P., & Obergfell, T. (2021). Combining food and energy production: Design of an agrivoltaic system applied in arable and vegetable farming in Germany. *Renewable and Sustainable Energy Reviews*, *140*, 110694. https://doi.org/https://doi.org/10.1016/j.rser.2020.110694

Valle, B., Simonneau, T., Sourd, F., Pechier, P., Hamard, P., Frisson, T., Ryckewaert, M., & Christophe, A. (2017). Increasing the total productivity of a land by combining mobile photovoltaic panels and food crops. *Applied Energy*, *206*, 1495–1507. https://doi.org/https://doi.org/10.1016/j.apenergy.2017.09.113

Wang, G. G., & Shan, S. (2008). Review of Metamodeling Techniques in Support of Engineering Design Optimization, 415–426. https://doi.org/10.1115/DETC2006-99412

Wicksteed, P. H. (1906). Pareto. Manuale di Economia Politica, con una Introduzione alla Scienza Sociale. *The Economic Journal*, *16*(64), 553–557. https://doi.org/10.2307/2221479

Zadeh, L. (1963). Optimality and non-scalar-valued performance criteria [Conference Name: IEEE Transactions on Automatic Control]. *IEEE Transactions on Automatic Control*, *8*(1), 59–60. https://doi.org/10.1109/TAC.1963.1105511

Zhang, J., & Xing, L. (2017). A Survey of Multiobjective Evolutionary Algorithms. *2017 IEEE International Conference on Computational Science and Engineering (CSE) and IEEE International Conference on Embedded and Ubiquitous Computing (EUC)*, *1*, 93–100. https://doi.org/10.1109/CSE-EUC.2017.27

Zhen-Yu, Y., & Yin-Fu, J. (2019). Optimization-Based Evolutionary Polynomial Regression | SpringerLink. Retrieved June 24, 2024, from https://link.springer.com/chapter/10.1007/978-981-13-3408-5_5

Zhou, Y., Xiang, Y., Chen, Z., He, J., & Wang, J. (2019). A Scalar Projection and Angle-Based Evolutionary Algorithm for Many-Objective Optimization Problems. *IEEE Transactions on Cybernetics*, *49*(6), 2073–2084. https://doi.org/10.1109/TCYB.2018.2819360

Zitzler, E., Laumanns, M., & Thiele, L. (2001, May). *SPEA2: Improving the strength pareto evolutionary algorithm* (tech. rep.) (Artwork Size: 21 p. Medium: application/pdf). [object Object]. https://doi.org/10.3929/ETHZ-A-004284029